약학박사학위논문

암 환경에서 IL-21 에 의한 자연 살해 세포의 기능 저하 회복에 관한 연구

Studies on Interleukin-21 mediated reversal of natural killer cell exhaustion in tumor microenvironment

2017 년 8 월

서울대학교 대학원
분자의학 및 바이오제약학과 면역학 전공
서 형 석

Abstract

Studies on Interleukin-21 mediated reversal of natural killer cell exhaustion in tumor microenvironment

Seo, Hyungseok
Laboratory of Immunology
Department of Molecular Medicine and Biopharmaceutical Sciences
The Graduate School
Seoul National University

During cancer immunoediting, tumor cells with spontaneous loss of Major Histocompatibility Complex (MHC) class I expression tend to gradually increase in the tumor microenvironment by preferentially escaping from immune surveillance of cytotoxic T cells even though MHC class I-deficient tumors have been historically considered to be susceptible to NK cell-dependent cytotoxicity. Recent studies demonstrated that most NK cells found in the tumor microenvironment of advanced cancers are defective, releasing the malignant MHC class I-deficient tumors from NK cell-dependent immune control. Here, I showed that an NKT cell-ligand loaded tumor-antigen expressing APC (Antigen Presenting Cell)-based vaccine effectively eradicated these advanced tumors that are not curable with a single immunotherapy. In this process, I found that the co-expression of Tim-3 and PD-1 marks functionally exhausted NK cells in advanced tumors and that MHC class I downregulation in tumors was closely associated with the induction of NK cell exhaustion in tumor-bearing mice as well as in cancer patients. Furthermore, the recovery of NK cell function by IL-21 was critical

for the anti-tumor effect of the vaccine against these advanced tumors. These results reveal the process involved in the induction of NK-cell dysfunction in advanced cancers and provide a guidance for the development of strategies for cancer immunotherapy.

Keywords: Natural Killer cell, Exhaustion, Cancer Immunotherapy, Immune checkpoint, IL-21, MHC class I

Student number: 2012-24146

Table of Contents

List of Figures

Abbreviations

Ab	Antibody
Ag	Antigen
APC	Antigen presenting cell
αGC	alpha-galactosylceramide
CD	Cluster of differentiation
CFSE	Carboxyfluorescein diacetate succinimidyl ester
CTL	Cytotoxic T lymphocyte
ELISA	Enzyme-linked immunosorbent assay
FACS	Fluorescence activated cell sorting
FSC	Forward scatter
GrazB	Granzyme B
IFN-γ	Interferon-gamma
IL-	Interleukin-
i.p.	Intraperitoneal
i.v	Intravenously
MHC	Major Histocompatibility Complex
Mo	Monocyte
NK	Natural Killer
PMBC	Peripheral blood mononuclear cell
s.c.	Subcutaneously
sgRNA	single guide Ribonucleic acid

SSC	side scatter
STAT	signal transducer and activator of transcription
TdLn	Tumour draining lymph node
TNF	Tumour necrosis factor

Introduction

MHC class I loss or downregulated tumour cells on cancer patients

Although a number of anti-cancer immunotherapies are currently being investigated in clinical trials, one of the major obstacles in treating advanced cancer is that tumour cells escape host immune responses via the downregulation of MHC class I such as beta 2 microglobulin and heavy chain gene of class I **(Figure 1)**[1, 2]. The malignant transformation and subsequent selection of highly metastatic cells by the immune system result in the loss of MHC class I in the neoplasm, contributing to tumour evasion from immunosurveillance by cytotoxic T lymphocytes (CTLs). Because CTLs cannot attack the MHC class I-deficient tumour cells. MHC class I downregulation or loss helps tumour cells evade the conventional CTLs dependent immune responses. Although It simultaneously impose another, the NK cell-associated immunosurveillance, activated by the 'missing self' signal, the downregulation of MHC class I in tumours induces NK cell dysfunction, leading to the outgrowth of MHC class I-deficient tumours **(Figure 2)**[3, 4]. However, the underlying mechanisms involved in the induction of NK cell dysfunction by MHC class I-deficient tumour cells and the best way to overcome the tolerogenic tumour microenvironment in advanced cancer remain to be elucidated [5]. Early studies indicated that the activation of NK cells is regulated by the integration of signals derived from activating and inhibitory receptors expressed on the cell surface [6]. In the presence of MHC class I on target cells, inhibitory NK cell receptors are triggered, leading to the inhibition of target cell lysis [7]. In contrast, upon the down-regulation of MHC class I on target cells, signals from activating receptors take precedence over those from inhibitory receptors, resulting in the lysis of target cells [8]. Paradoxically, however, MHC class I deficiency has been reported in a number of advanced cancers and is associated with NK cell dysfunctionality, which forms the basis for a long-standing question regarding cancer immune evasion [4, 5, 9, 10].

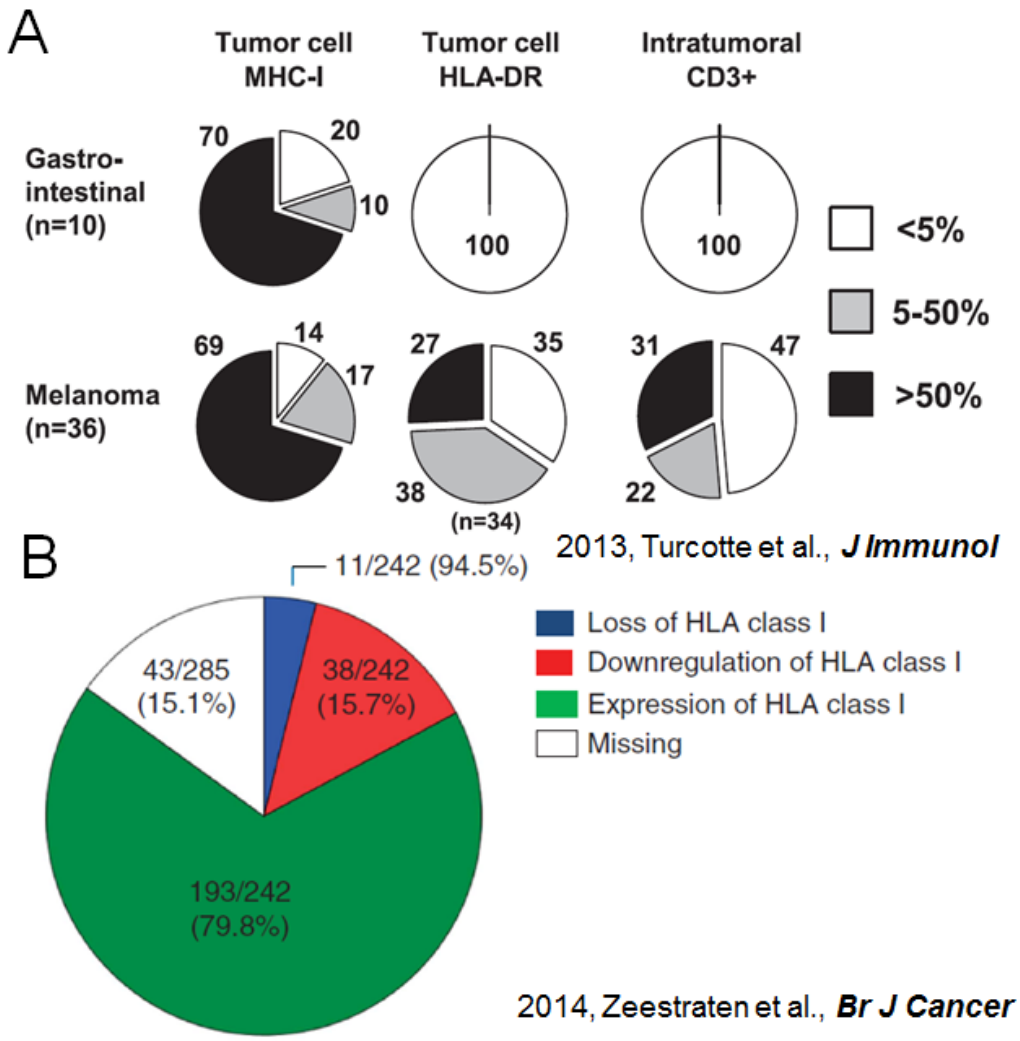

Figure 1. MHC class I downregulation or loss on tumour cells.

(A) Immunohistochemistry of MHC class I and HLA-DR expression on gastro intestinal and melanoma visceral metastases[2]. (B) Frequencies of HLA class I expression in colon cancer patients[11].

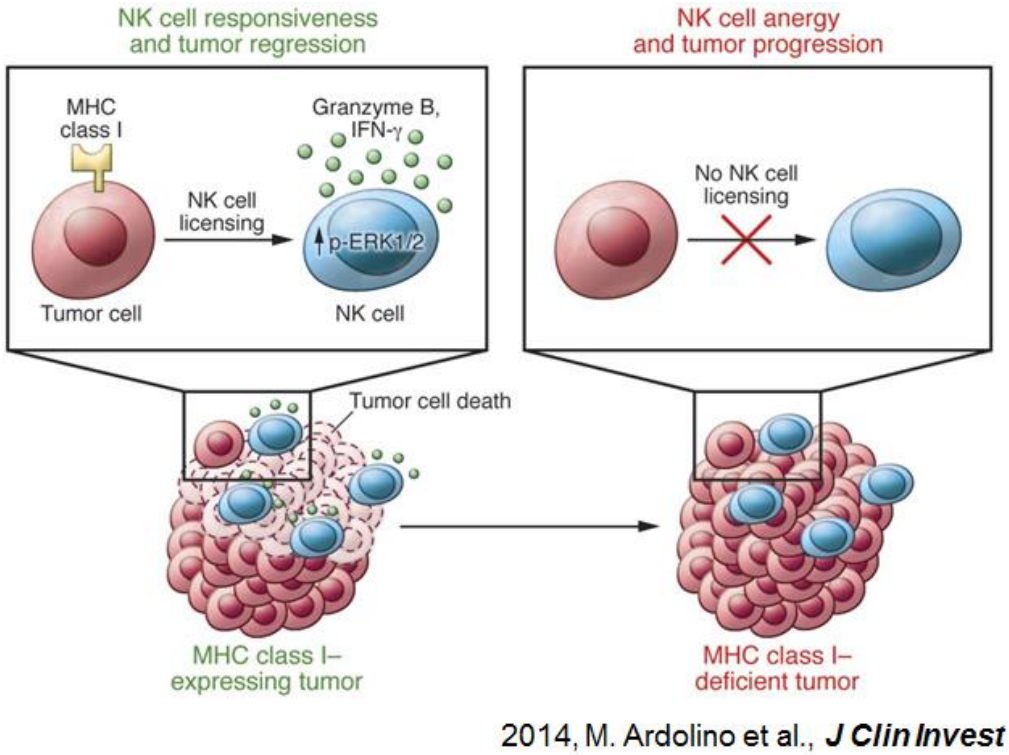

Figure 2. MHC class I deficient tumour induce NK cell anergy

When tumour cells lose MHC class I expression, which can occur for a variety of reasons, they disarm the function of NK cells, which become “unlicensed”

Immune exhaustion and checkpoint blockade

Co-inhibitory receptors, such as programmed death 1 (PD-1) and T cell immunoglobulin and mucin domain 3 (Tim-3), play a crucial role in mediating T cell exhaustion in both viral infections and tumours **(Figure 3)**[12, 13]. At first, Tim-3 and PD-1 were initially known to be activation markers of T cells. However, recent studies have demonstrated that Tim-3 and PD-1 co-expression is a marker of exhausted T cells after repeated TCR stimulation during chronic infection or in the tumour microenvironment [13, 14]. Checkpoint blockade, which inhibits PD-1, Tim-3 signals, is a recent hot issue in cancer therapy that has shown surprising results in various cancers and infection patient groups [15]. Recently, FDA approved immune checkpoint blockers are in clinical development such as monoclonal antibodies that target the PD-1, Tim-3 [16, 17]. However, Checkpoint blockaded therapy is not always effective, and we need a complete understanding of the specific mechanisms which contribute to resistance or efficacy [18].

Currently, clinical and experimental evidence suggests that a $CD8^+$ T cell, which infiltrated in tumour burden, is most favourable prognostic index of checkpoint blocker responses[19, 20]. The expression of these receptors has been identified in diverse immune cell populations including T cells, B cells, myeloid cells and macrophages[21]. Although previous studies demonstrated that the PD-1/PD-L1 and Tim-3/ligands of Tim-3 signalling down-modulated the cytotoxicity of NK cells against tumour cells [22, 23], their expression on NK cells was not well documented until a few recent human studies reported PD-1 and Tim-3 expression on NK cells of cancer patients[24, 25].

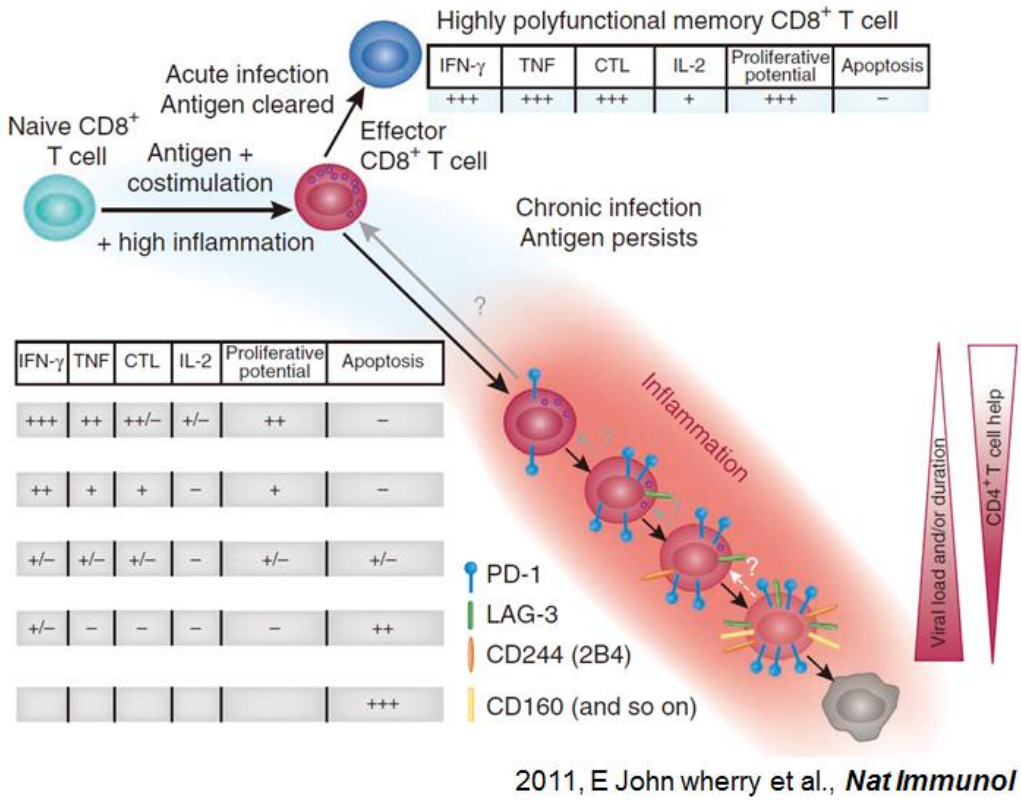

Figure 3. Hierarchical T cell exhaustion during chronic infection.

During initial infection, naive T cell are primed by antigen, costimulation and inflammation and differentiate into effector T cell. During chronic infection, infection persists after the effector phase. As antigen and/or viral load increases. T cell progress through stages of dysfunction, losing effector functions and other properties in a hierarchical manner. T cell exhaustion is also accompanied by a progressive increase in the amount and diversity of inhibitory receptors expressed[26].

Interleukin-21 and NK cell

Various cytokines tested in clinical trial activated NK cell and induce antitumor effects[27]. For example, IL-2, IL-12, IL-15, IL-18 and IL-21 activates T cells and NK cells[28]. However, short half-life, substantial toxicity, poor responses in cancer patients limit their clinical admiration[29]. So, we need to understand cytokine biology in tumor microenvironments, and which cytokine could be more effective for eradicating tumor cells than others. IL-21 is a cytokine mainly produced by follicular helper T cell (T_{FH} cell), T helper 17 cells (T_H17) and natural killer T cell (NKT cell)[30]. The IL-21 receptor (IL-21R) is expressed on NK, B, T, and dendritic cells **(Figure 4)** [31]. Several studies have reported that IL-21 acts directly on viral antigen-specific $CD8^+$ T cells to enhance their functional responses and to limit exhaustion during chronic viral infection [32, 33, 34]. IL-21 promotes the maturation of NK cell progenitors and activates the anti-tumour effects of NK cells through the NKG2D pathway [35, 36]. In addition, IL-21 activates cytotoxic programs in both $CD8^+$ T and NK cells, thus providing potent cytotoxic effector arms against cancer cells [37]. Based on these studies, several clinical trials are currently underway [30]. IL-21 transduces various molecular signals such as STAT, PI3K and MAPK pathways[31]. IL-21 stimulation leads to the activation of STAT1, STAT3 and STAT5 on NK cells[38]. IL-21 enhances the cytotoxicity of $CD8^+$ T cells by upregulating T-bet and IFN-γ via STAT1[39, 40]. In addition to STAT1 pathway, IL-21 stimulation also activate PI3K-AKT pathways. These pathways are known to enhance proliferation[41] and upregulate T-bet via Foxo1 phosphorylation[42, 43].

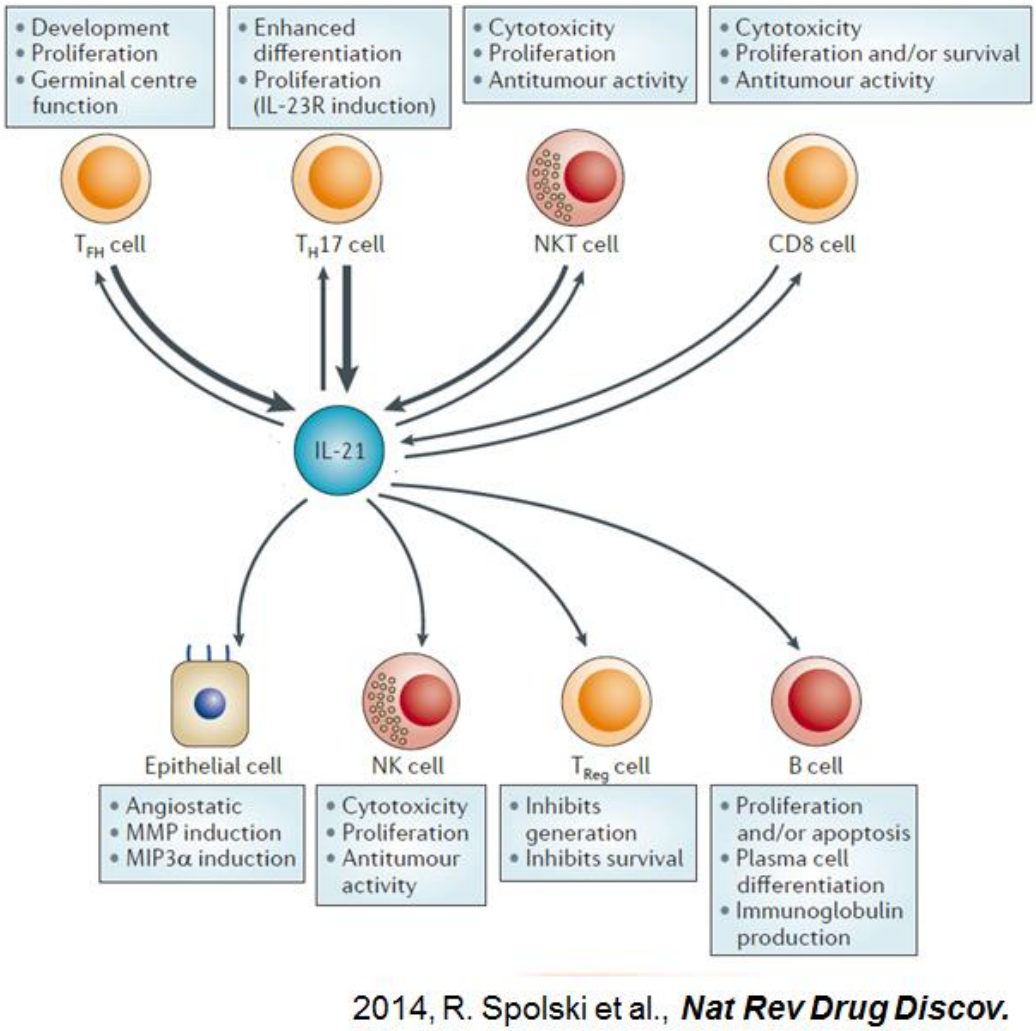

Figure 4. Sources of IL-21 and its cellular targets.

IL-21 is produced by CD4+ T cell populations, with the highest production by T_{FH} cells and T_H17 cells, and slightly lower levels produced by natural killer T cells. CD8+ T cells can also produce IL-21. IL-21 exerts actions on multiple lymphoid and myeloid populations as well as on epithelial cells[30].

Purpose of this study

Our laboratory have previously reported that an invariant natural killer T (NKT) cell ligand, alpha-galactosylceramide (αGC), loaded on a tumour antigen (tAg)-expressing B cell- and monocyte-based vaccine (B/Mo/tAg/αGC) elicited diverse anti-tumour immune responses **(Figure 5)** [44, 45, 46]. Initially, our study aimed to demonstrate whether B/Mo/tAg/αGC induces antitumor effects in MHC class I-deficient tumor-bearing hosts. Although recent studies have reported that MHC class I-deficient tumors induce NK cell dysfunction [3, 4],

In this study, I found that B/Mo/tAg/αGC effectively eradicated otherwise resistant MHC class I–deficient tumour cells by activating NKT cells and inducing tumour antigen-specific cytotoxic T cell responses. Whereas MHC class I-deficient tumour cells selectively induced Tim-3^+PD-1^+ NK cells with impaired cytotoxicity in the tumour microenvironment, B/Mo/tAg/αGC vaccination restored the cytotoxic capacity of NK cells. In addition, I found that the functional recovery of exhausted Tim-3^+PD-1^+ NK cells by vaccination was solely dependent on the activation of PI3K-AKT-Foxo1 and STAT1 signalling pathways by IL-21 produced by NKT cells. Accordingly, the addition of recombinant IL-21 restored the function of intratumoural Tim-3^+PD-1^+ NK cells both in animal models and in human cancer patients.

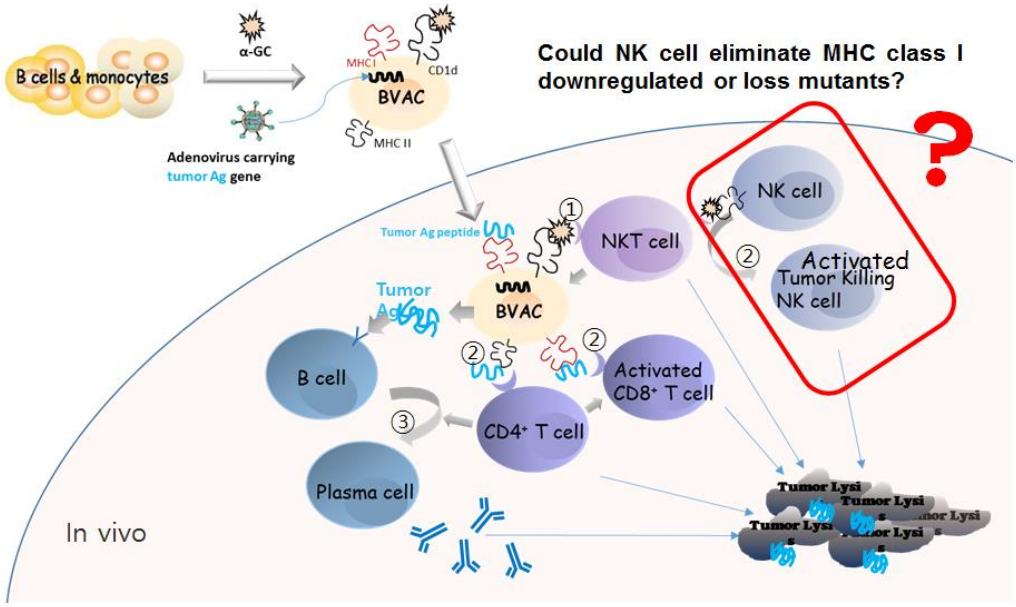

Figure 5. Mode of action of NKT ligand loaded tumour antigen expressing B cell and monocyte based vaccine.

An invariant natural killer T (NKT) cell ligand, alpha-galactosylceramide (αGC), loaded on a tumour antigen (tAg)-expressing B cell- and monocyte-based vaccine (B/Mo/tAg/αGC) elicited diverse anti-tumour immune responses such as CD4, CD8 T cell and NK cell responses and tumour antigen specific antibodies production.

Materials and Methods

Mice

Female C57BL/6 and BALB/c mice were purchased from Charles River Laboratories (Seoul, Korea). The Jα281$^{-/-}$ mice were kindly provided by Dr. Doo-Hyun Chung (Seoul National University, Seoul, Korea). The Rag 1$^{-/-}$ mice were purchased from the Jackson Laboratory (Bar Harbor, ME, USA). The IFN-γ-reporter-eYFP (GREAT) mice on a C57BL/6 background were kindly provided by Dr. Richard M. Locksley (University of California, San Francisco, USA). The IL-2Rγ$^{-/-}$Rag2$^{-/-}$ mice were purchased from Taconic (Germantown, New York, USA) All mice were used at 6 to 10 weeks of age and were bred and maintained in the specific pathogen-free vivarium of Seoul National University. All animal experiments were approved by the Institutional Animal Care and Use Committee (IACUC; SNU-130104-1-3) at Seoul National University.

Human Samples

The human tumour tissue and normal tissue specimens from patients with colorectal, melanoma and bladder cancer were cut into small pieces at the Department of Surgery, Shinchon Severance Hospital, Yonsei University College of Medicine.

Human peripheral blood was obtained from healthy volunteers, and informed consent was granted from all donors. Peripheral blood mononuclear cells (PBMCs) were prepared by Ficoll-Hystopaque (Sigma-Aldrich, USA) density gradient centrifugation. The collection of human samples and all human experiments were approved by the ethical committee of Seoul National University and Shinchon Severance Hospital, Yonsei University College of Medicine (IRB No. 1309/001-023).

Reagents and antibodies

The antibodies for flow cytometry and western blot assays were purchased from Biolegend (San Diego, CA, USA), eBioscience (San Diego, CA, USA), BD Bioscience (San Jose, CA, USA) and Cell Signaling Technology (Danvers, MA, USA). Antibody information can be found in **Table 1**. All microbeads (CD3ε, CD11b, CD19, CD14, B220, EpCam and Biotin) for lymphocyte depletion or selection were purchased from Miltenyi Biotec (Bergish Galdbach, Germany). The antibodies for in vivo depletion (Asialo GM-1, NK1.1 (PK136), CD4 (GK1.5), CD8 (2.43), IL-21R (4A9) and IFN-γ (XMG 1.2)), were prepared in the laboratory or purchased from Biolegend or BioXcell. The recombinant mouse IL-2, mouse IL-21, human IL-2, human IL-21, ULBP2 and human NKp46 antibodies were purchased from R&D Systems. Chemical inhibitors, including S31-201, Fludarabine, LY294002, and PD98059, were purchased from Selleckchem (Houston, TX, USA)

Cell line generation and culture

The TC-1, CT26, MC38, K562 and HeLa cells were purchased from ATCC. The cells were cultured in DMEM or IMEM (GIBCO) supplemented with 10% FBS (GIBCO) and 1% penicillin-streptomycin. The optimized sgRNA constructs, targeting H-2K^b (Exon 3: AGCCGTCGTAGGCGTACTGCTGG), H-2D^b (Exon 3: AGTCACAGCCAGACATCTGC TGG), mouse Beta 2 microglobulin (Exon 2: TCACGCCACCCACCGGAGAATGG) and human Beta 2 microglobulin (Exon 1: GAGTAGCGCGAGCACAGCTAAGG), and the Cas9 expression construct, pRGEN-Cas9-CMV, were obtained from ToolGen (Seoul, Korea). The TC-1 H-2K^b,D^b, MC38 H-2K^b,D^b, CT26 Beta 2 microglobulin and HeLa Beta 2 microglobulin knock out cell lines were generated by transfection with the indicated sgRNA construct and pRGEN-Cas9-CMV using Lipofectamine 2000 (Invitrogen) according to the manufacturer's protocol. MHC class I-deficient cells were sorted by a T7E1 assay with single cell selection or with a FACSARIA III (BD Bioscience). For primary cell cultures, mouse primary cells were cultured in RPMI (GIBCO) medium supplemented with 10% FBS (GIBCO) and 1% penicillin-

streptomycin (Lonza). Human primary cells were cultured in X-VIVO15 medium (Lonza) that was supplemented with 1% penicillin-streptomycin (Lonza). For NK cell culture, a low dose (1~2 ng/ml) of rIL-2 was added to the culture medium for cell survival. All cell lines were found to be negative for mycoplasma contamination.

Construction of recombinant adenoviruses

All adenoviral vectors were constructed by Cellid, Inc. (Seoul, Korea). To construct the adenoviral vector that expressed the HPV antigen E6/E7 gene in the E1 region of adenovirus, we first constructed a pShuttle-CMV vector (Agilent Technologies, CA, USA) that expressed the HPV antigen E6/E7 protein. The newly generated pShuttle-CMV-E6E7 vector was co-transformed with the pAdeasy-1 adenovirus vector (Agilent Technologies, CA, USA) in which a portion of the Ad type 5 fibre was replaced by a portion of the Ad type 35 fibre (Adk35), yielding the plasmid pAdk35-E6E7. This recombinant plasmid was transfected into human embryonic kidney 293 cells to generate the Adk35-E6E7 adenovirus.

B/MoAdk35-E6E7/αGC and B/Mo/αGC preparation

Splenocytes were isolated from C57BL/6 or BALB/c mice. The granulocytes and RBCs were removed by Ficoll (Sigma-Aldrich) density gradient centrifugation. After the depletion of $CD3\varepsilon^+$ and $DX5^+$ cells from the cell population using anti-mouse CD3ε and anti-mouse DX5 microbeads, the $CD11b^+$ cells and $B220^+$ cells were purified using anti-mouse CD11b and anti-mouse B220 microbeads (all from Miltenyi Biotec). Isolated B cells and monocytes (1:1 ratio mixture) were transduced with the adenoviral vector in a 90-min, 2800-rpm centrifugation step at room temperature, and the cells were subsequently incubated for an additional 18 h (for the B/Mo/αGC preparation this step was skipped). αGC (KRN7000, Enzo Life Science, Japan) was loaded into the prepared B cells and monocytes for NKT activation based on our laboratory previous studies [44, 45, 46, 47].

Transplant tumour and therapeutic tumour models

Conventional subcutaneous indicated tumours were generated by s.c. injection in the right flank. Tumour growth was measured using a metric calliper 2-3 times a week. In some experiments, tumour cells were injected s.c. in the flank after being resuspended in Matrigel with reduced matrix growth factor (BD Bioscience). For the therapeutic tumour model, $1x10^4$-$1x10^6$ of the indicated tumour cells were subcutaneously injected into the left flanks of the mice on day 0. After the randomized and blinded allocation of all tumour-bearing mice, the indicated vaccine or cytokine was administered at various time points. For the TC-1 lung metastasis model, $1x10^5$ cells were injected i.v. into the tail vein after resuspension in 100 μl PBS. Tumour formation was monitored using IVIS Spectrum microCT and Living Image (ver. 4.2) software (PerkinElmer, Cambridge, UK). An MMPSense 680 probe (PerkinElmer; 2 nmol per 150 ml in PBS) was used to facilitate tumour monitoring. For adoptive transfer into the IL-2R$\gamma^{-/-}$Rag2$^{-/-}$ mice, tumour cells were subcutaneously injected into the left flank of the mice, and on the next day, the indicated cells were transferred by i.v. injection into the tail vein. In addition, the transferred groups of No treatment, Tim-3$^-$ PD-1$^-$ NK cells and IL-21-treated Tim-3$^+$ PD-1$^+$eYFP$^-$ NK cells were injected daily with rIL-21 (2 μg) via i.p. for 4 days. To deplete NK1.1$^+$, CD4$^+$, CD8$^+$ cells, 300 μg of GK1.5, 2.43, PK136 or control antibodies were injected i.p. twice weekly into the mice the day before tumour implantation. To block IL-21R or IFN-γ, anti-IFN-γ (500 μg/mouse) or anti-IL-21R (300 μg/mouse) or both were injected i.p. nine days after tumour implantation, and two days later, the indicated cellular vaccine was injected along with the neutralizing antibodies.

Antibody staining and flow cytometry analysis

Dead cells were excluded by staining with Fixable Viability Dye (eBioscience, CA, USA) following the manufacturer's instruction. The cells were stained with the specified antibodies in 50 μl of FACS buffer (PBSN+1% FBS). Intracellular staining for cytokines was performed after surface staining with

the Cytofix/Cytoperm kit (BD Bioscience). For transcription factor staining, the Foxp3/Transcription factor staining buffer set (eBioscience) was used. In addition, for the intracellular staining of p-ERK, p-AKT, p-FOXO1, pSTAT1 and pSTAT3, the cells were fixed with IC fixation buffer and permeabilized with 1 ml ice-cold 90% methanol on ice for at least 30 minutes in the dark after surface staining. The samples were acquired with a FACSCalibur or FACSARIA III instrument (BD Bioscience), and the data were analysed with Flow Jo software (Three Star).

Tumour-infiltrating lymphocyte preparation

Tumours were dissociated using the gentleMACS Dissociator (Miltenyi Biotec). The dissociated tumour samples were further digested in 10% FBS with RPMI medium containing 300 μg/ml collagenase D (Roche), 20 μg/ml hyaluronidase (Sigma Aldrich) and 20 μg/ml DNase I (Sigma Aldrich). After filtering through a 40-μm nylon mesh, single cell suspensions were counted and used for the experiments.

In vitro cytotoxicity assay

Effector $CD8^+$ cells were prepared from vaccinated mouse splenocytes and stimulated with the $E6_{41-50}$ [EVYDFARDL]/$E7_{49-57}$ [RAHYNIVTF] peptide mixture for 5 days. After the 5-day stimulation, $CD8^+$ T cells were isolated using anti-mouse CD8 microbeads (Miltenyi Biotec) and cocultured with ^{51}Cr-labeled TC-1 tumour cells for 4 hours. The CTL activity was calculated by the release of 51Cr in the culture supernatants through the specific lysis of TC-1 target cells, as measured by a Wallac 1480 Wizard automatic γ-counter (PerkinElmer). NK cells were prepared from vaccinated mouse splenocytes or infiltrating lymphocytes from MHC class I-deficient tumour-bearing mice or human infiltrating NK cells from cancer patients by FACSARIA II or FACSARIA III sorting. Next, various numbers of NK cells were cocultured with ^{51}Cr-labeled TC-1 H-$2K^b$,D^b KO cells or K562 cells. The NK cell cytotoxicity was calculated by 51Cr release in the culture supernatants

through the specific lysis of TC-1 H-2K^b,D^b KO target cells or K562 cells, as measured by a Wallac 1480 Wizard automatic γ-counter (PerkinElmer). To assay the cytokine release from NK cells, $3x10^4$~$1x10^6$ cells were stimulated in flat-bottomed, high protein-binding plates (Corning) that were coated with anti NK1.1, ULBP-2 Fc protein or hNKp46 antibodies for 5 h in the presence of 1 μg/ml GolgiPlug (BD) before staining the cells for intracellular IFN-γ, perforin or granzyme B. In some experiments, CD107a was added during cell stimulation. When NK cells were cocultured with tumour cells, the tumour cells were irradiated (5000 rads) using a gamma irradiator (GC 3000 Elan) at the National Center for Inter-university Research Facilities (NCIRF) at Seoul National University.

Immunoblot analysis

The cytoplasmic fractions of cells were prepared as follows: cells were washed once with ice-cold phosphate-buffered saline (PBS) and collected by centrifugation at 3,000 rpm for 5 min. The cells were resuspended in 10 mM HEPES, pH 7.9, 10 mM KCl, 0.2 mM EDTA, 1 mM DTT, 0.25 mM PMSF, and proteinase inhibitor cocktail. After incubation on ice for 5 min, NP-40 was added to a final concentration of 0.25%. The mixtures were vortexed at high speed for 10 seconds. The extracts were collected by centrifugation at 13,000 rpm for 1 minute. The supernatants were collected as cytoplasmic extracts.

Immunohistochemistry

Tumour tissues were fixed in 4% paraformaldehyde; paraffin-embedded tissue sections (4 mm) were deparaffinized, dehydrated, and treated with 3% hydrogen peroxide to block endogenous peroxidase. Slides were incubated with the primary antibody (Anti-MHC class 1 H-2 D^b antibody, Abcam Inc, MA, USA). Slides were then washed with phosphate buffered saline (PBS), incubated with HRP secondary antibody, and washed again in PBS; colour

was developed using the AEC substrate. The slides were counterstained with haematoxylin.

Enzyme-linked immunosorbent assay

The following cytokines were measured in mouse serum using an ELISA kit according to the manufacturer's instructions: IL-21 (eBioscience), IFN-γ, TNF-α and IL-4 (BD Bioscience, San Jose, CA, USA).

Statistics

Statistical comparisons were performed using the Prism 6.0 software (GraphPad Software).

two-tailed unpaired Student's t test: Figure 13, 15, 16A, 17A-C, 18C, 20B-C, 21A, 24A-B, 27, 32B-G, 33A, 34B-C and 35A-B,

two-way ANOVA with Bonferroni multiple comparison tests: Figure 6A-C, 7A, 11A-F, 12A, 21B, 22B, 26A, 26C, 28B, 29A-C, 30A-D, 31B, 35B and 36

log-rank (Mantel-Cox) test: Figure 7 C and 12B-D,

Results

Effects of the vaccine for advanced tumours

To investigate whether B/Mo/tAg/αGC has anti-tumour effects on large established tumours, I first developed a B/Mo/tAg/αGC vaccine expressing the E6/E7 tumour Ag of human papillomavirus-associated cancer (B/Mo/E6E7/αGC). I found that B/Mo/E6E7/αGC elicited activation of NKT **(Figure 6A)** and NK cells **(Figure 6B)** and induced antigen-specific CTL responses **(Figure 6C)**. A single vaccination on day 7 with B/Mo/E6E7/αGC was successful for the treatment of mice bearing small E6/E7-expressing TC-1 tumours **(Figure 7A)** and protected mice against tumour re-growth **(Figure 8)**. Multiple vaccinations at late time points effectively eradicated large established TC-1 tumours **(Figure 7B)**, and lung metastases derived from TC-1 tumour cells were efficiently eradicated by vaccination with B/Mo/E6E7/αGC **(Figure 7C-D)**. To investigate the effects of B/Mo/E6E7/αGC on MHC class I-downregulated tumours, I analysed the kinetics of H-2K^b and H-2D^b expression on tumours. A gradual downregulation of H-2K^b and H-2D^b was observed with tumour progression **(Figure 9A-B)**. The cytotoxic activity of NK cells gradually increased during tumour progression, while the cytotoxicity of CD8$^+$ T cells gradually decreased **(Figure 9C-D)**. The cytotoxicity of NK cells was inversely correlated with the expression of H-2K^b, D^b on tumours, whereas that of CD8$^+$ T cells was positively correlated with the expression of H-2K^b, D^b **(Figure 9E)**. This observation prompted us to address whether MHC class I-deficiency can affect NK cell functions [9]. To this end, I established H-2K^b, D^b-deficient or beta2-microglobulin (β_2m)-deficient tumours **(Figure 10A-B)**. The progression of tumour growth in the respective syngeneic mice was comparable between WT and MHC class I-deficient tumours **(Figure 10C-E)**.

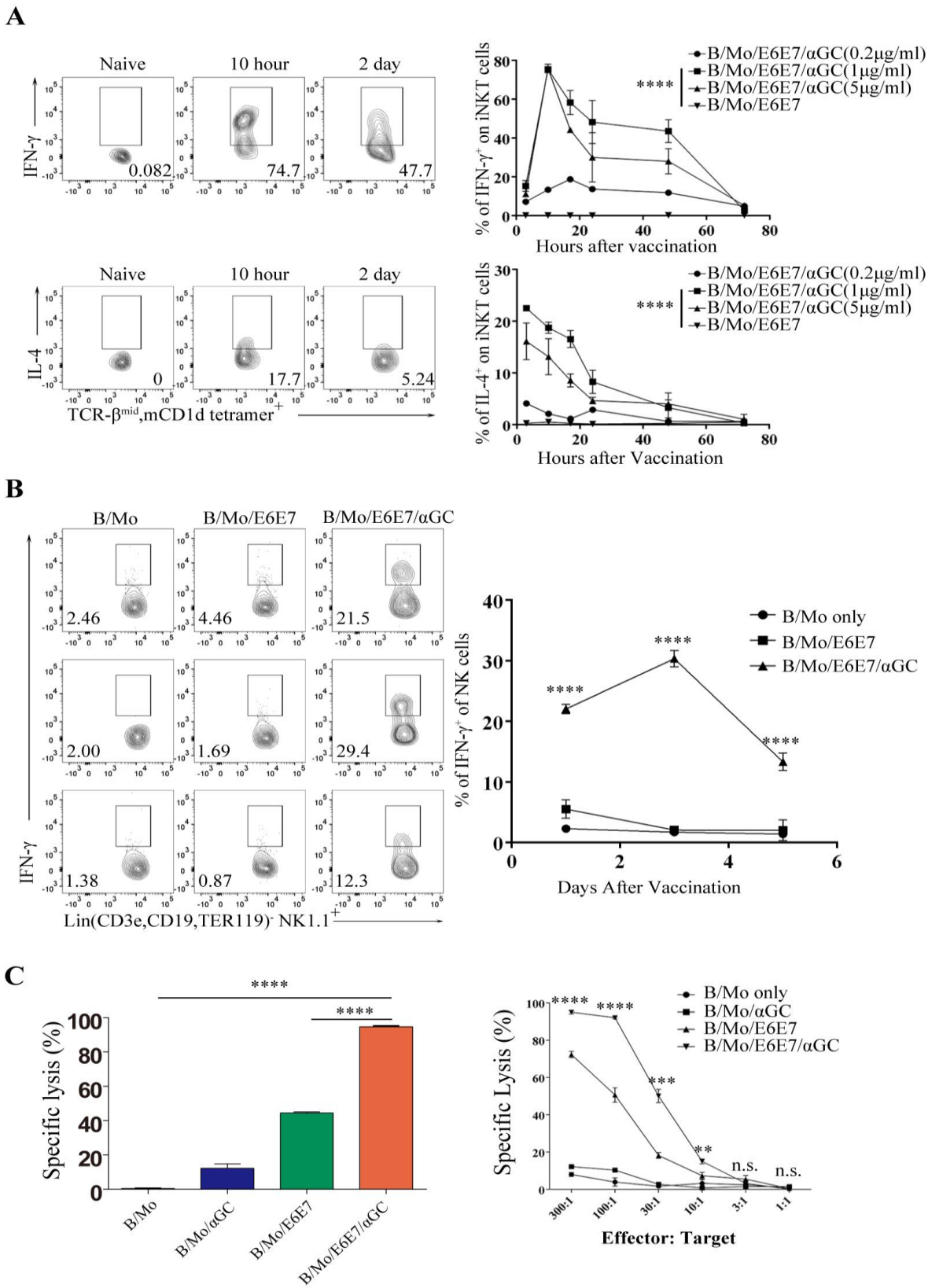
A
Naive
10 hour
2 day
IFN-γ
0.082
74.7
47.7
IL-4
0
17.7
5.24
TCR-β^mid,mCD1d tetramer+
B/Mo/E6E7/αGC(0.2μg/ml)
B/Mo/E6E7/αGC(1μg/ml)
B/Mo/E6E7/αGC(5μg/ml)
B/Mo/E6E7
****
% of IFN-γ+ on iNKT cells
Hours after vaccination
% of IL-4+ on iNKT cells
Hours after Vaccination
B
B/Mo
B/Mo/E6E7
B/Mo/E6E7/αGC
2.46
4.46
21.5
2.00
1.69
29.4
1.38
0.87
12.3
Lin(CD3e,CD19,TER119)- NK1.1+
B/Mo only
% of IFN-γ+ of NK cells
Days After Vaccination
C
Specific lysis (%)
B/Mo
B/Mo/αGC
B/Mo/E6E7
B/Mo/E6E7/αGC
Specific Lysis (%)
Effector: Target
300:1
100:1
30:1
10:1
3:1
1:1
n.s.

Figure 6. NKT ligand-loaded tumour antigen-presenting B cell- and monocyte-based vaccine induces NKT, NK and CD8 T cell responses.

(A) The cytokine profiles of liver iNKT cells were assessed in B/Mo/Adk35-E6E7/αGC-injected mice at various times. The levels of IL-4 and IFN-γ were detected by flow cytometry. (**B)** Twelve days after TC-1 WT cell implantation, IFN-γ production by tumour-infiltrating NK cells was assessed in B/Mo-, B/Mo/Adk35-E6E7- and B/Mo/Adk35-E6E7/αGC-injected mice. (**C)** C57BL/6 mice were vaccinated with the indicated form of B/Mo. One week later, in vivo CTL assays were performed by injecting CFSE-labelled syngeneic targets. $CFSE^{high}$, peptide pulsed target; $CFSE^{low}$, peptide unpulsed control. In vitro assays were performed using vaccinated mice splenocytes that were restimulated with the HPV16 E6/E7 peptide mixture (E6: EVYDAFRDL, E7: RAHYNIVTF), and cytotoxicity against TC-1 cells was measured using a standard ^{51}Cr release assay. The data shown are from at least 2 individual experiments with similar results. The data in A, B and C were analysed by two-way ANOVA with Bonferroni multiple comparison tests. *P<0.05, **P<0.01, ***P<0.001, ****P<0.0001.

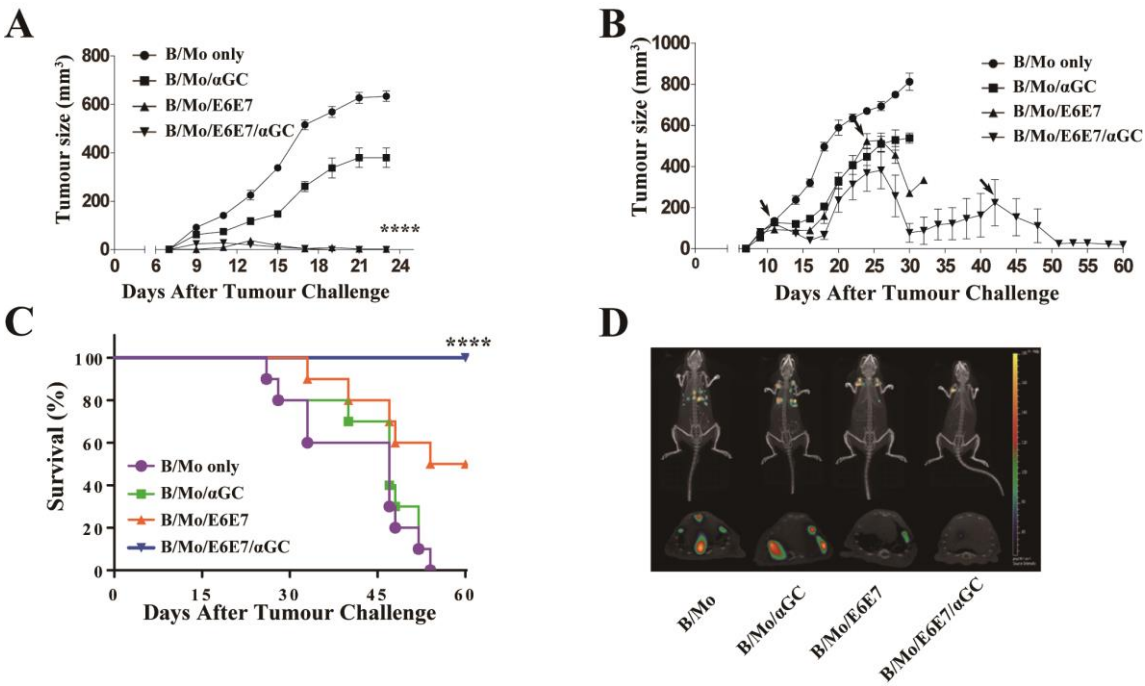

Figure 7. Anti-tumour effects of BVAC-C. (A) Each group of mice (n=6) was vaccinated with the indicated cellular vaccine at day 6 after TC-1 tumour s.c. injection ($1x10^5$) at day 0. **(B)** Each group of mice (n=8) was vaccinated with the indicated cellular vaccine at day 10, 24 and 41 after TC-1 tumour s.c. injection ($5x10^5$) at day 0. The tumour size was measured three times weekly. **(C-D)** Each group of mice (n=10) was vaccinated with the indicated cellular vaccine at day 7, 14 and 21 after TC-1 tumour i.v. injection ($1x10^5$) at day 0. **(D)** In vivo imaging of TC-1 metastatic mice (day 40) treated with metalloproteinase. The data in A were analysed by two-way ANOVA with Bonferroni multiple comparison tests. The data in C were analysed using a log-rank (Mantel-Cox) test (conservative) *P<0.05, **P<0.01, ***P<0.001, ****P<0.0001. The data are representative of three independent experiments that included three to ten mice per group. All values represent the mean ± s.e.m.

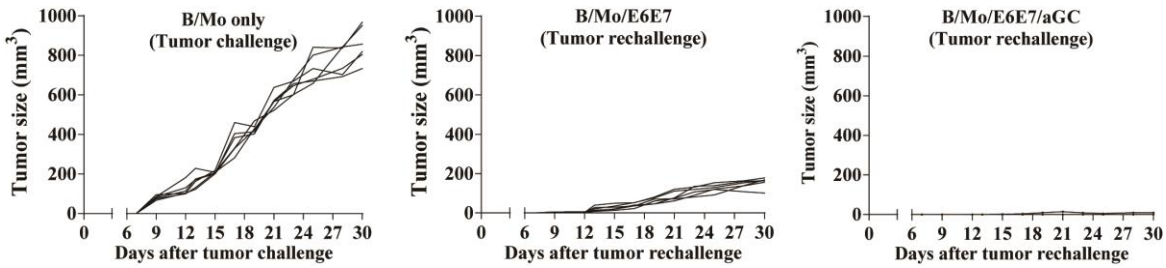

Figure 8. Memory anti-tumour responses induced by vaccination. Tumour-free mice from Fig. 7A and naïve mice (n=6) were vaccinated with the indicated cellular vaccine at day 6 after TC-1 tumour s.c. rechallenge ($1x10^5$) on the opposite flank as on day 0. The data shown are from at least 2 individual experiments with similar results.

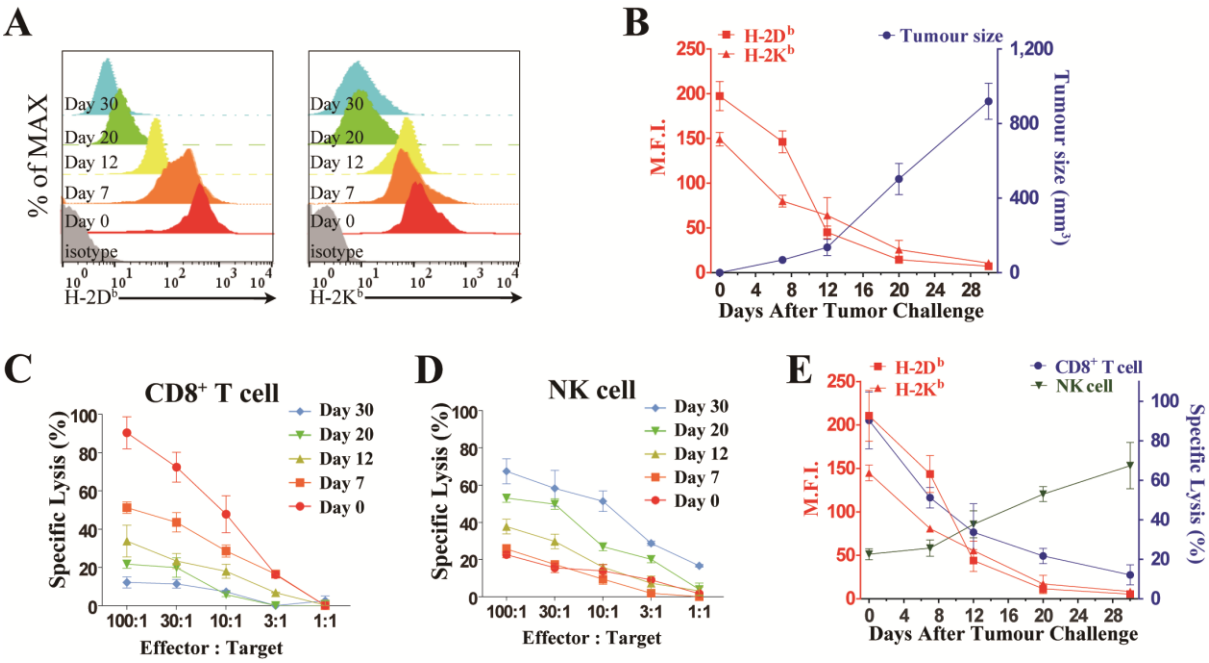

Figure 9. MHC class I downregulation affects anti-tumour immunity. (**A**) Expression of H-2K^b, D^b on tumours. C57BL/6 mice were implanted in the flank with 1x10^5 TC-1 cells (Day 0 indicates in vitro cultured tumour cells). **(B)** H-2K^b, D^b expression (E) is shown with tumour size. **(C-D)** Each graph depicts the specific lysis of extracted TC-1 cells at different time points. CD8$^+$ T cells and NK cells were isolated from the spleens of B/Mo/ E6E7/αGC-immunized mice at day 1 and 7 as effector cells. **(E)** The data presented in G-H reassembled with the H-2K^b, D^b level on tumours and the percentage of specific lysis when the effector-to-target ratio was 30:1.

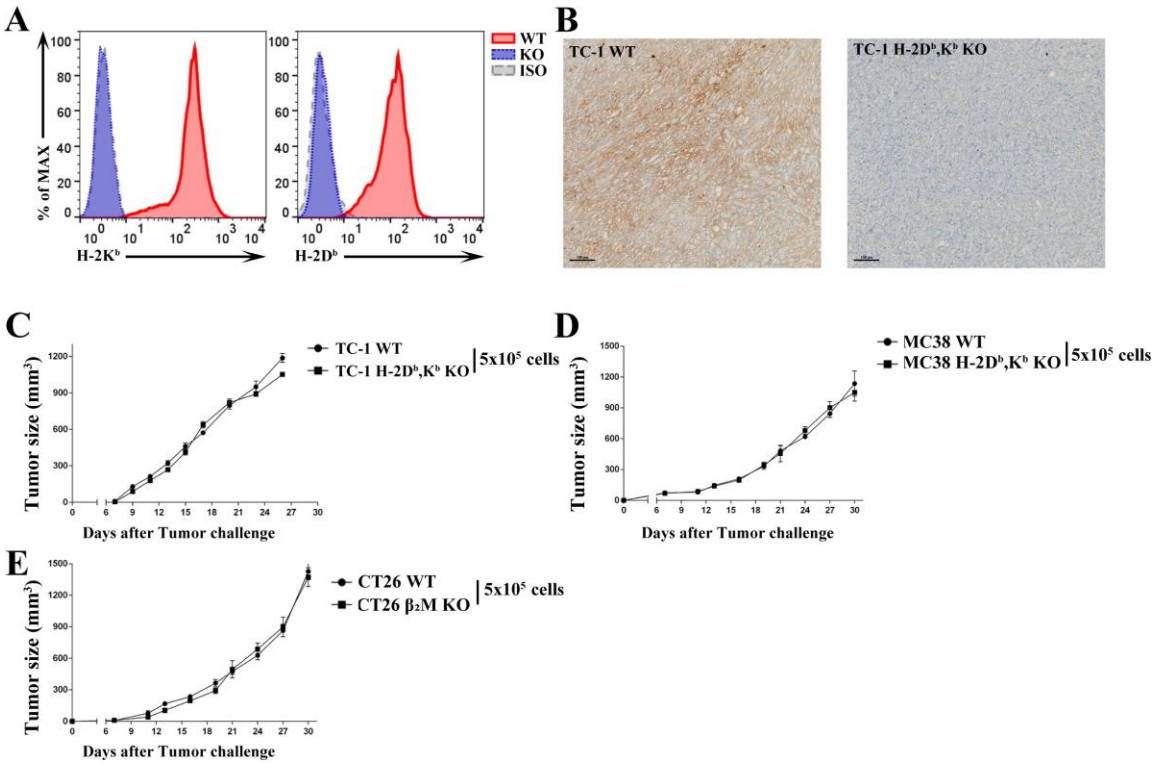

Figure 10. H-2D^b, K^b or Beta 2 microglobulin knock out tumour cells. **(A)** The expression levels of H-2D^b and H-2K^b on TC-1 WT or TC-1 H-2K^b,D^b KO cells were measured by flow cytometry. **(B)** The H-2D^b expression level in TC-1 WT or TC-1 H-2K^b,D^b KO-bearing mouse tumour (n=5) sections was detected by immunohistochemistry (H2-D^b: brown, tumour: blue, Scale bar: 100μm). **(C-E)** The tumour size was measured after s.c. implantation of the indicated tumour cells. The data shown are from at least 2 individual experiments with similar results.

Anti-tumour effects of B/Mo/αGC on MHC class I-deficient tumours

Several mouse and human studies have shown that NKT cell activation triggers anti-tumour immune responses by enhancing NK cell activation [48, 49]. To verify that this was also the case with MHC class I-deficient tumours, mice were injected with αGC-loaded B cells and monocytes (B/Mo/αGC) followed by MHC class I-deficient tumour inoculation. The B/Mo/αGC administration resulted in a significant reduction in the growth of MHC class I-deficient tumours compared with B/Mo **(Figure 11A-C)**. I also found that treatment with anti-NK1.1 or anti-asialo GM1 significantly reversed the inhibition of tumour growth, which indicated that the anti-tumour immunity was dependent on NK and NKT cells (**Figure 11D-F)**. However, human malignant primary tumours are well known for their heterogeneous MHC class I expression levels [2, 11]. Therefore, I hypothesized that NKT cell ligand-loaded tumour antigen-expressing vaccination can eradicate both MHC class I-sufficient and MHC class I-deficient tumour cells by inducing adaptive and innate immune responses. MHC class I-sufficient tumours could be eradicated by adaptive immune responses, such as $CD8^+$ T cells, and MHC class I-deficient tumours could be eradicated by innate immune responses, such as the response of NK cells. To address this hypothesis, I established a heterogeneous tumour model in which a mixture of MHC class I sufficient- and MHC class I-deficient tumour cells was inoculated at different ratios. The data revealed that the vaccine regimen induced complete tumour eradication and a long-lasting cure in 90% of the mice bearing heterogeneous tumours and thus contain up to 10% MHC class I-deficient TC-1 tumour cells **(Figure 12A-B)**. B/Mo/E6E7/αGC administration induced robust tumour eradication and durable cures in >70% of the mice bearing heterogeneous tumours, which contained 20% MHC class I-deficient TC-1 tumour cells. In contrast, B/Mo/E6E7 or B/Mo/αGC administration elicited weaker anti-tumour responses and reduced survival rates **(Figure 12C)**. Antibody depletion experiments showed that $CD8^+$ T and

NK cells were crucial for heterogenic tumour eradication and led to reductions in the survival rates **(Figure 12D)**. These results indicate that the vaccine regimen is effective against the heterogeneous tumours by inducing both adaptive and innate immune responses.

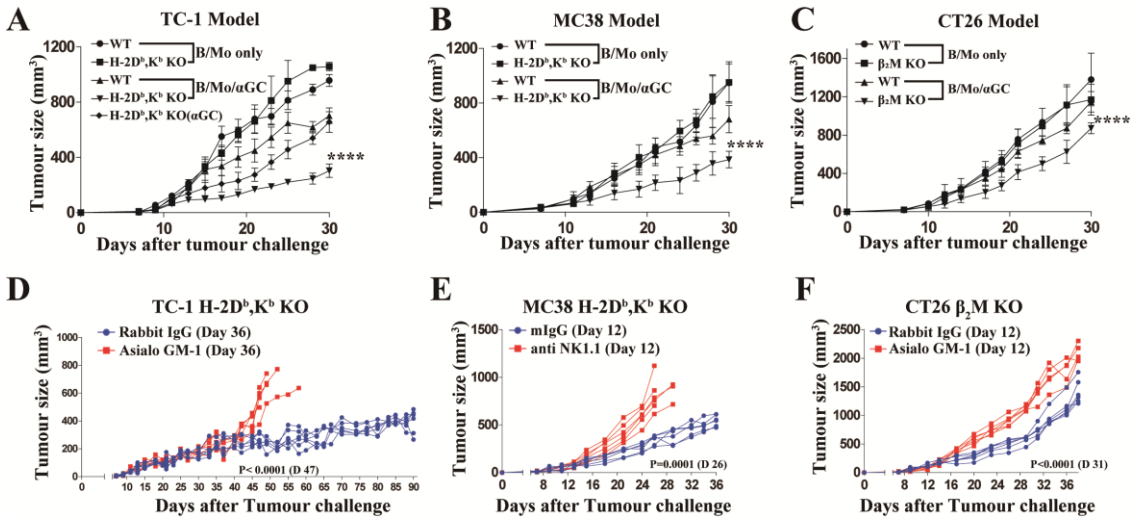

Figure 11. **Eradication of MHC class I deficient tumour by NK and NKT dependent manner.** (**A-C)** Subcutaneous growth of WT and MHC class I KO tumour cells (TC-1, MC38: H-2K^b, D^b KO, CT26: β2m KO) in each group of mice (n=6) treated with B/Mo (1x10^6), B/Mo/αGC (1x10^6) and αGC (1 μg) every 7 days. (**D-F)** Subcutaneous growth of the indicated tumour cells in each group of mice (n=6) treated with B/Mo (1x10^6) or B/Mo/αGC (1x10^6) every week. The tumour bearing mice were treated control IgG, anti-NK1.1 (PK136) or anti-asialo GM-1 to deplete NK cells on day 36 (TC-1) or day 12 (MC38 and CT26). A-F were analysed by a two-way ANOVA with Bonferroni multiple comparison tests. *P<0.05, **P<0.01, ***P<0.001, ****P<0.0001. The data are representative of three independent experiments that included six to ten mice per group. All values represent the mean ± s.e.m.

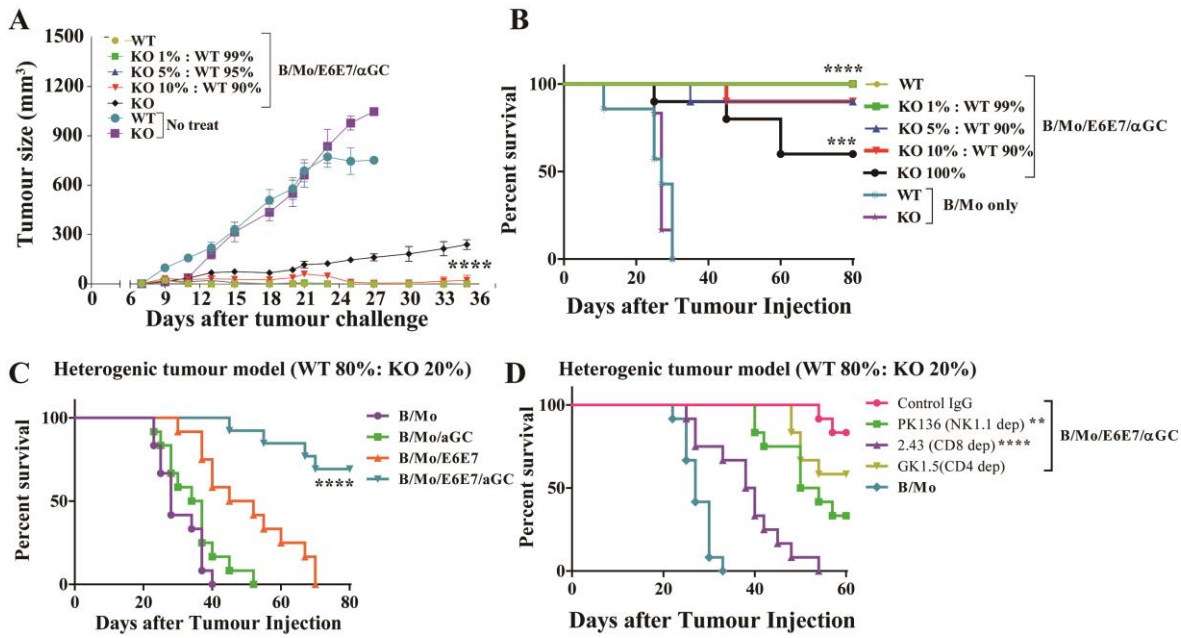

Figure 12. **Eradication of heterogeneous tumours by induced adaptive and innate immune responses. (A-B)** Each group of mice (n=10) was vaccinated with the indicated cellular vaccine every 7 days after s.c. injection of the indicated mixed (WT and MHC class I-deficient tumour) or solid (TC-1) tumours ($1x10^5$) at day 0. **(C-D)** Survival over time with depleting antibodies for indicated cells (PK136 for NK cells depletion, 2.43 for $CD8^+$ T cell depletion and GK1.5 for $CD4^+$ T cell depletion) administered i.p.1d before initiation of the vaccination. Each group of mice (n=12) was vaccinated with the indicated cellular vaccine every 7 days after s.c. injection of the mixed (TC-1 WT and MHC class I-deficient tumour ratio = 80:20) tumours ($1x10^5$) at day 0. A were analysed by a two-way ANOVA with Bonferroni multiple comparison tests. The data in B-D were analysed by a log-rank (Mantel-Cox) test (conservative) *P<0.05, **P<0.01, ***P<0.001, ****P<0.0001. All values represent the mean ± s.e.m.

MHC I deficient tumours induce Tim-3 and PD-1 on NK cells

Although recent studies have demonstrated that MHC class I-downregulation or deficiency in tumour cells induces NK cell anergy, NKT cell ligand-loaded APC-based tumour Ag-expressing vaccination efficiently induced the eradication of tumours containing MHC class I-deficient cells. From this perspective, I hypothesized that NK anergy in mice bearing MHC class I-deficient tumours might have been restored by the vaccination. To investigate this possibility, I analysed the cell surface marker expression pattern and cytotoxic function of NK cells in MHC class I-deficient tumour microenvironments. Recent studies have suggested that Tim-3 expression is a marker of NK cell activation or exhaustion [23, 24]. I observed that Tim-3 expression on tumour-infiltrating NK cells was dramatically accelerated in mice bearing H-2K^b,D^b-deficient tumours compared with WT tumour-bearing mice, and most Tim-3$^+$ NK cells co-expressed PD-1 **(Figure 13)**. The levels of Tim-3 and PD-1 expression on NK cells in the spleen were very low, regardless of the MHC class I expression on tumours, but those in tumour-draining lymph nodes were slightly increased in mice bearing H-2K^b, D^b-deficient tumours compared with WT tumour-bearing mice, although this increase was not statistically significant **(Figure 14)**. The expression levels of NK cell-activating receptors, including Ly49D, DNAM-1, CD69, and CD160, were significantly higher in Tim-3$^+$ PD-1$^+$ NK cells compared with Tim-3$^-$PD-1$^-$ cells. The expression of NK cell-inhibitory receptors such as NKG2A/C/E, KLRG1, TIGIT and 2B4 was comparable between the groups, but Ly49A was downregulated in Tim-3$^+$PD-1$^+$ NK cells **(Figure 15)**. To investigate whether the tumours could directly induce the expression of Tim-3 and PD-1 on NK cells, I cocultured purified NK cells with tumour cells. When NK cells were cocultured with WT tumour cells, Tim-3 was slightly induced starting on day 1, and PD-1 was not induced until day 5. However, when NK cells were cocultured with MHC class I-deficient tumour cells, Tim-3 was highly induced starting on day 1, and PD-1 was induced on day 5 **(Figure 16A)**. To analyse whether soluble factors produced by tumours could

induce Tim-3 and PD-1, NK cells were both cocultured with MHC class I-deficient tumour cells using a transwell system and in tumour-conditioned medium. The expression of Tim-3 and PD-1 on NK cells was induced when the NK cells and MHC class I-deficient tumours were directly cocultured **(Figure 16B)**. In human NK cells, Tim-3 expression was rapidly upregulated upon coculture with β_2m-deficient HeLa cells compared with NK cells cocultured with WT HeLa cells **(Figure 17A)**. Human NK cell-activating receptors, including NKG2D, DNAM-1 and CD69, and the inhibitory receptor 2B4 were significantly upregulated on Tim-3^+ NK cells compared to Tim-3^- cells. However, expression of the inhibitory receptor KLRG1 was significantly downregulated in Tim-3^+ NK cells **(Figure 17B)**. The levels of PD-1 on Tim-3^+ NK cells were slightly higher than those on Tim-3^- cells **(Figure 17C)**. These results collectively suggest that Tim-3^+PD-1^+ NK cells express higher levels of activating receptors.

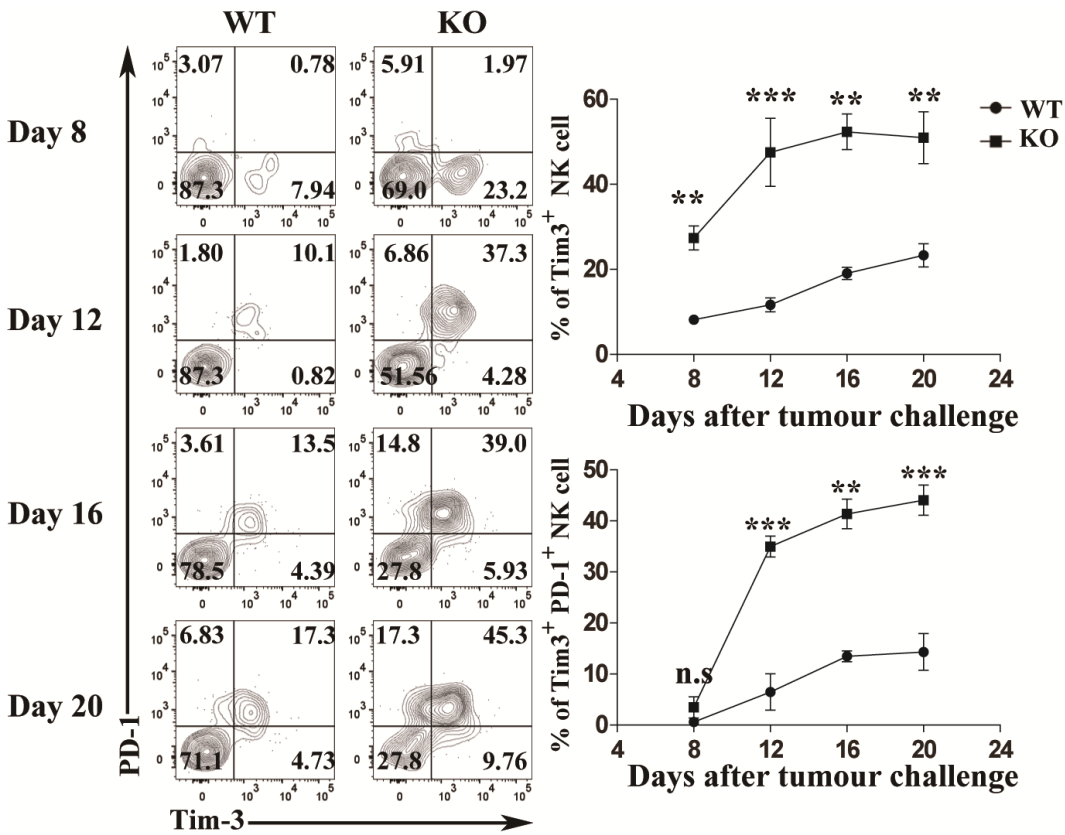

Figure 13. Natural killer cells in MHC class I-deficient tumours exhibit accelerated Tim-3 and PD-1 expression. The kinetic expression levels of Tim-3 and PD-1 on tumour-infiltrating natural killer cells from TC-1 WT or H-2K^b,D^b KO tumour-bearing mice (n=5) were analysed by flow cytometry. The data in A were analysed by a two-tailed unpaired Student's t test. *P<0.05, **P<0.01, ***P<0.001. All values represent the mean ± s.e.m.

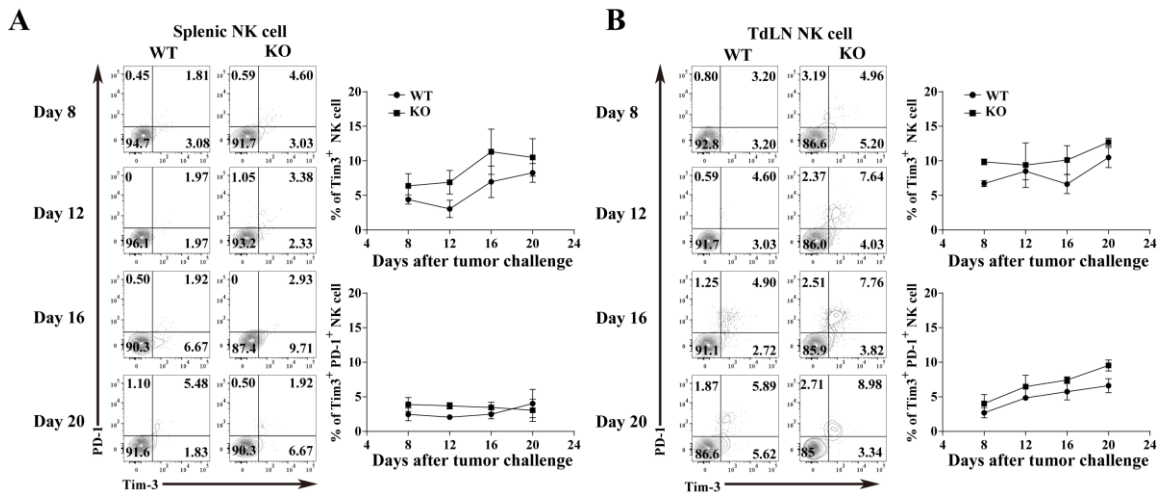

Figure 14. Tim-3 and PD-1 expression on natural killer cells in the indicated organs. The kinetic expression levels of Tim-3 and PD-1 on natural killer cells from TC-1 WT or H-2K^b,D^b KO tumour-bearing mice (n=5) were analysed by flow cytometry.

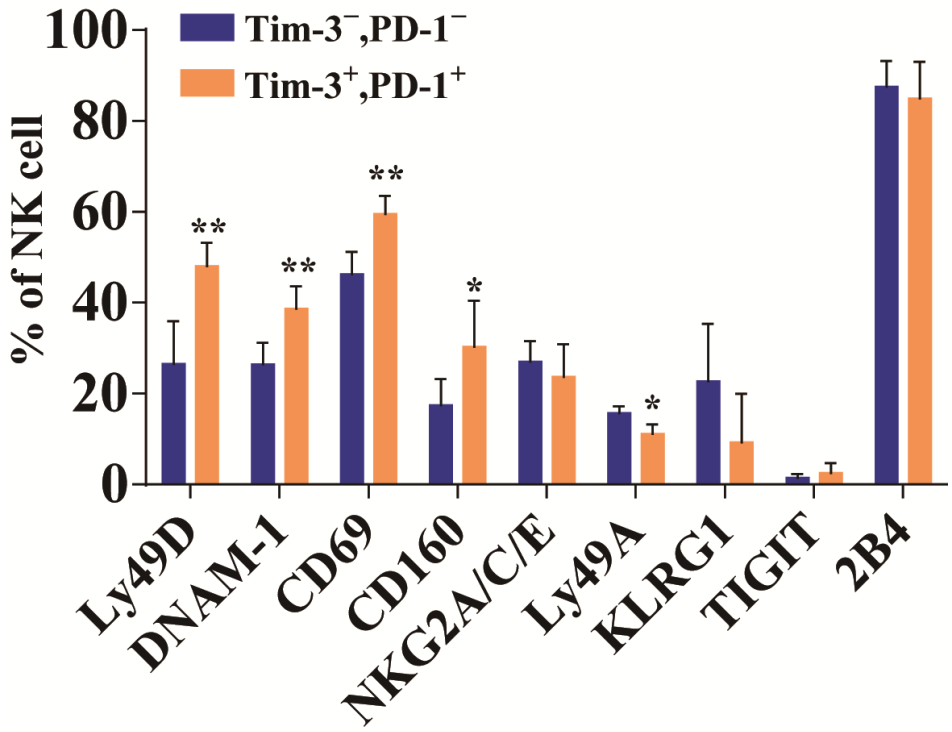

Figure 15. Various inhibitory and activation molecule expression on indicated NK cells. Tim-3^{+}PD-1^{+} or Tim-3^{-}PD-1^{-} NK cells from TC-1 H-2K^{b},D^{b} KO tumours were stained with antibodies for the activating receptors Ly49D, DNAM-1, CD69 and CD160 or the inhibitory receptors NKG2A/C/E, Ly49A, KLRG1, TIGIT and 2b4.

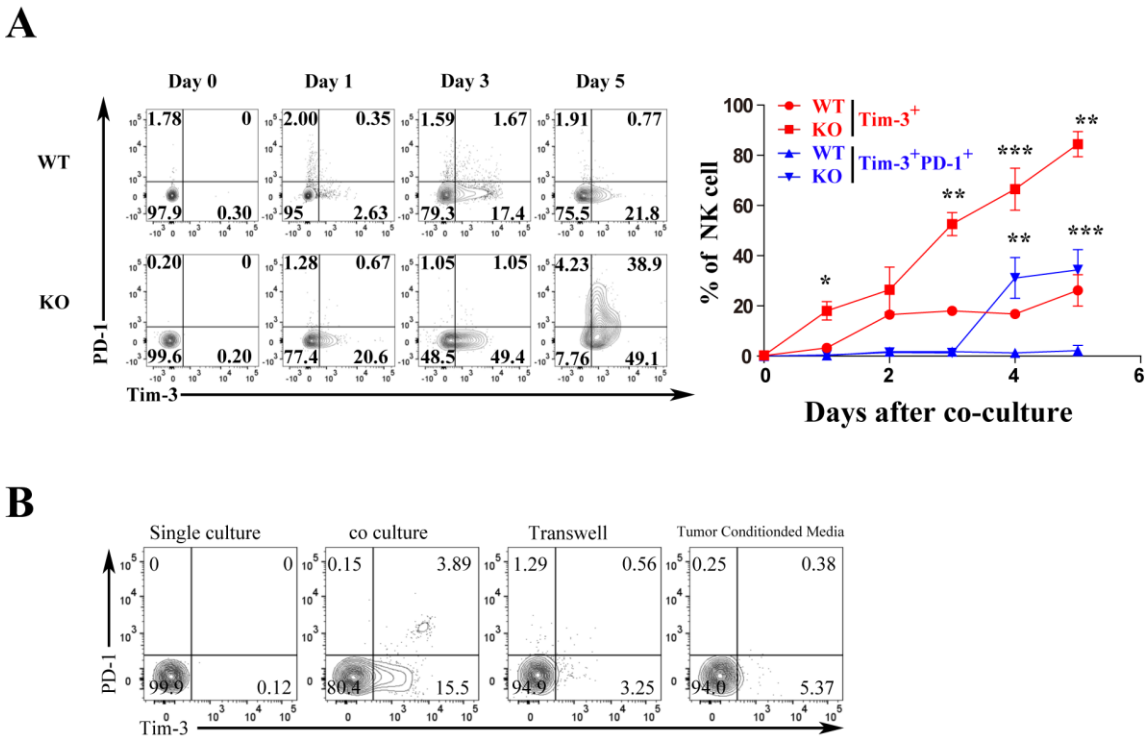

Figure 16. Tim-3 and PD-1 expression on NK cells in vitro. (A) The daily kinetic Tim-3 and PD-1 expression levels on NK cells were analysed after MC38 WT or H-2K^b,D^b KO tumour cells were cocultured in vitro with splenic NK cells from C57BL/6 mice. **(B)** The expression levels of Tim-3 and PD-1 on NK cells were assessed after coculture with TC-1 H-2K^b,D^b KO cells via transwell or the addition of tumour-conditioned medium. The data were analysed using a two-tailed unpaired Student's t test *P<0.05, **P<0.01, ***P<0.001.

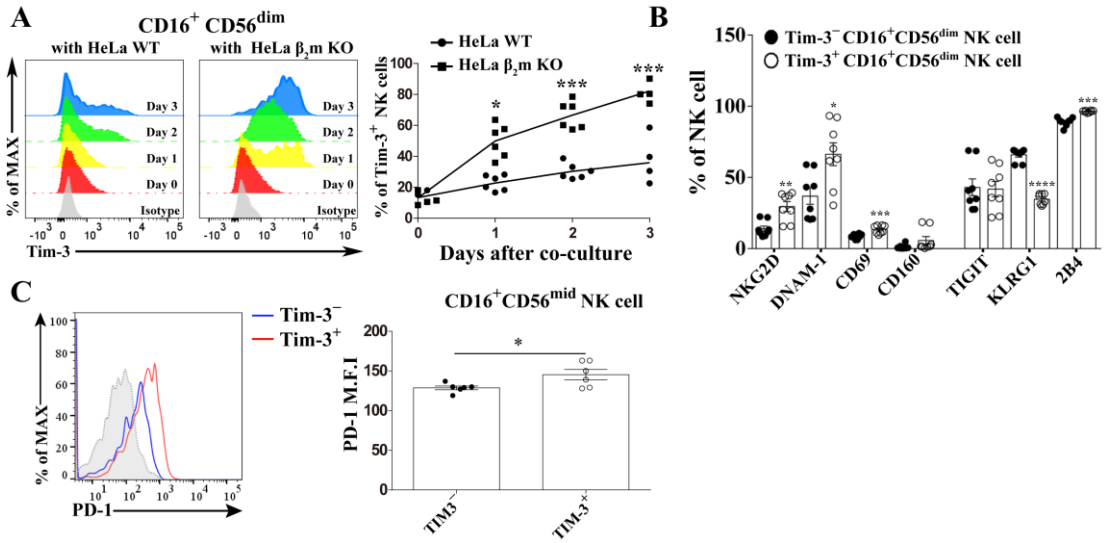

Figure 17. Human Natural killer cells in MHC class I-deficient tumours exhibit accelerated Tim-3 and PD-1 expression. (A) The Tim-3 expression level on human NK cells was analysed after $CD16^{+}CD56^{dim}$ human NK cells (n=6) were cocultured with HeLa WT or β2m KO cells. **(B)** $Tim\text{-}3^{+}$ or $Tim\text{-}3^{-}$ human NK cells (n=8) cocultured with HeLa β2m KO cells for 3 days were stained with antibodies for the activating receptors NKG2D, DNAM-1, CD69 and CD160 or the inhibitory receptors TIGIT, KLRG1, 2B4 and PD-1 **(C).** The data in A, B and C were analysed by a two-tailed unpaired Student's t test. *P<0.05, **P<0.01, ***P<0.001. The data are representative of three independent experiments that included six to eight human PBMC samples. All values represent the mean ± s.e.m.

Tim-3$^+$ PD-1$^+$ NK cells are functionally exhausted in tumour.

Although Tim-3 and PD-1 were initially suggested to be activation markers of T cells, recent studies have demonstrated that Tim-3 and PD-1 co-expression is a marker of exhausted T cells after repeated TCR stimulation during chronic infection or in the cancer microenvironment [13, 14]. To investigate whether Tim-3$^+$ PD-1$^+$ NK cells induced by MHC class I-deficient tumours represent activated or exhausted NK cells, I analysed the effector functions of NK cell populations isolated from mice bearing WT or H-2K^b, D^b-deficient tumours. I determined that the frequency of IFN-γ^+ NK cells was remarkably decreased in tumour-infiltrating lymphocytes (TILs) and tumour-draining lymph nodes (TdLNs) of mice bearing H-2K^b, D^b-deficient tumours compared with those bearing WT tumours **(Figure 18C)**, although the frequency and number of NK cells were comparable between the two groups **(Figure 18A-B)**. ERK1/2 kinase is a crucial factor for the induction of cytokine production and cytotoxicity in NK cells [50]. The levels of phospho-ERK1/2 were significantly reduced in TIL NK cells from MHC class I-deficient tumour-bearing mice compared with TIL NK cells from WT tumour-bearing mice **(Figure 19A).**

To investigate the interrelationship between Tim-3 and PD-1 expression and function on NK cells, I analysed the kinetics of the expression of these receptors and the IFN-γ secretion of intratumoural NK cells from mice bearing WT and H-2K^b, D^b-deficient tumours. In mice bearing WT tumours, the expression of Tim-3 and PD-1 on intratumoural NK cells reached 50% at 28 days after tumour injection. In contrast, Tim-3 and PD-1 were expressed much more rapidly on intratumoural NK cells from mice bearing H-2K^b, D^b-deficient tumours than on intratumoural NK cells from mice bearing WT tumours, reaching up to 70% at 28 days after tumour injection. I also observed that IFN-γ production of intratumoural NK cells from both groups of mice sharply decreased in response to the increased expression of Tim-3 and PD-1 **(Figure 20A)**. Of note, among the NK cells isolated from MHC class I-deficient tumours, Tim-3$^+$ PD-1$^+$ NK cells

exhibited a dramatically reduced expression of effector molecules such as IFN-γ, CD107a, granzyme B and perforin compared with their Tim-3$^-$PD-1$^-$ counterparts **(Figure 20B)**. These results suggest that when NK cells are stimulated, Tim-3 and PD-1 are first expressed on NK cells as an activation signature. However, after persistent stimulation in the absence of MHC class I, Tim-3$^+$ PD-1$^+$ expression represented the exhausted NK cell population. In addition, T-bet expression on Tim-3$^+$PD-1$^+$ NK cells in H-2K^b,D^b-deficient tumours was also reduced compared with Tim-3$^-$PD-1$^-$ NK cells, whereas the expression of Eomes was somewhat increased on Tim-3$^+$PD-1$^+$ NK cells **(Figure 20C)**. Moreover, ERK1/2 phosphorylation was significantly decreased in Tim-3$^+$PD-1$^+$ NK cells **(Figure 21A)**. Consistent with their exhausted phenotype, the cytotoxicity of the Tim-3$^+$PD-1$^+$ NK cells against H-2K^b,D^b-deficient TC-1 tumours was much lower than the cytotoxicity exhibited by Tim-3$^-$ PD-1$^-$ NK cells **(Figure 21B)**. I also found that Tim-3$^+$PD-1$^+$ intratumoural NK cells in WT tumour-bearing mice had a similar exhausted phenotype, in accordance with the spontaneous downregulation of MHC class I on WT tumour cells **(Figure 19B)**.

To determine whether the PD-1/PD-L1 axis transmits negative signals on NK cells, I examined whether the tumour cells expressed PD-L1. My data showed that MC38 tumour cells had a high expression level of the PD-L1 molecule on their surface **(Figure 22A)**. To examine the effect of anti-PD-1 antibody on exhausted NK cells, I treated MC38 H-2K^b, D^b KO tumour-bearing mice, which were depleted of CD8$^+$ T cells by 2.43 mAb, with the anti-PD-1 antibody. This treatment significantly suppressed tumour growth in mice bearing MC38 H-2K^b, D^b KO tumours **(Figure 22B)**. Collectively, my data suggest that the PD-1/PD-L1 axis transmits negative signals on NK cells and that blocking the PD-1 signal could restore the anti-tumour effects of exhausted NK cells. When human NK cells were cocultured with β_2m-deficient HeLa cells, the IFN-γ and granzyme B levels in Tim-3$^+$ NK cells were gradually decreased after restimulation with the NKG2D ligand ULBP-2 **(Figure 23A)**. A gradual reduction in T-bet expression in Tim-3$^+$NK cells

was highly correlated with the pattern of IFN-γ production, whereas the expression pattern of Eomes was opposite that of T-bet **(Figure 23B)**. Altogether, these data suggest that repeated stimulation of NK cells by MHC class I-deficient tumours induces the functional exhaustion of NK cells marked by the co-expression of Tim-3 and PD-1 in mice and humans.

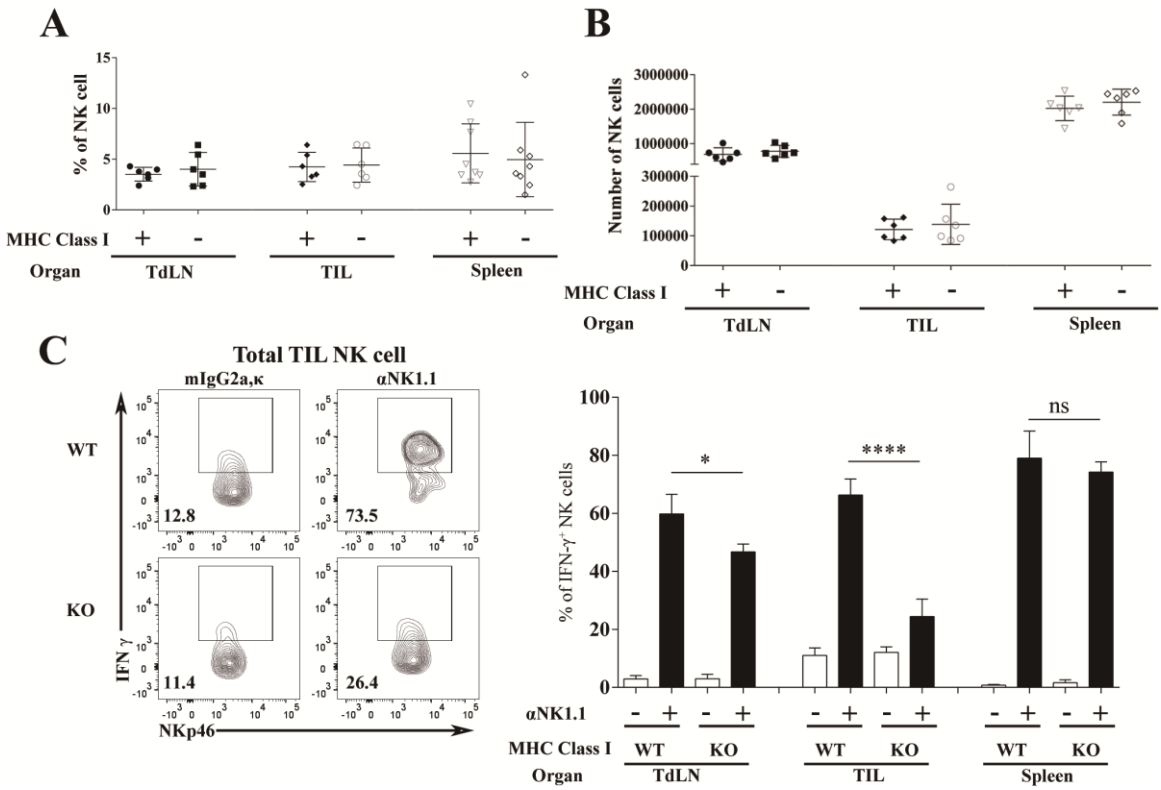

Figure 18. Percent, number and function of NK cells in MHC class I-deficient tumours. (A-C) Twelve days after TC-1 WT or H-2K^b,D^b KO cell implantation, **(A)** the percent and **(B)** number of NK cells were analysed in the indicated organs. (**C)** Lymphocytes from the indicated organs were restimulated in vitro with anti-NK1.1 or control IgG for 30 minutes, and IFN-γ production was then evaluated by flow cytometry. The data shown are from at least 2 individual experiments with similar results. The data in C were analysed using a two-tailed unpaired Student's t test. *P<0.05, **P<0.01, ***P<0.001, ****P<0.0001.

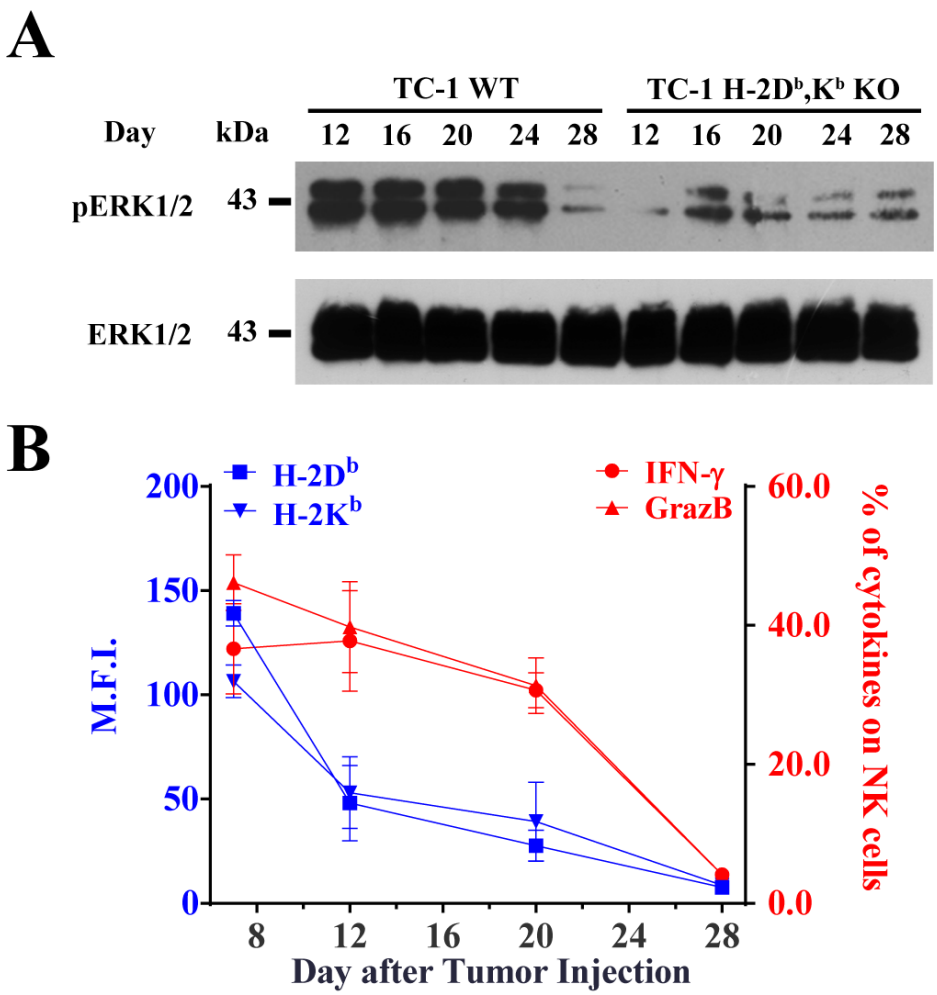

Figure 19. ERK activation kinetics and functional analysis of TC-1 WT or H-2K^b,D^b tumour-infiltrating NK cells. (A) ERK1/2 phosphorylation was detected by western blot analysis after restimulation in vitro with anti-NK1.1 or control IgG antibody for 30 minutes with TC-1 WT or H-2K^b,D^b KO implantation (5x10^5)-infiltrating NK cells at different time points **(B)** The expression of H-2K^b, D^b , IFN-γ and Granzyme B on tumour cells or intratumoural NK cells from mice bearing TC-1 WT tumours was measured over time.

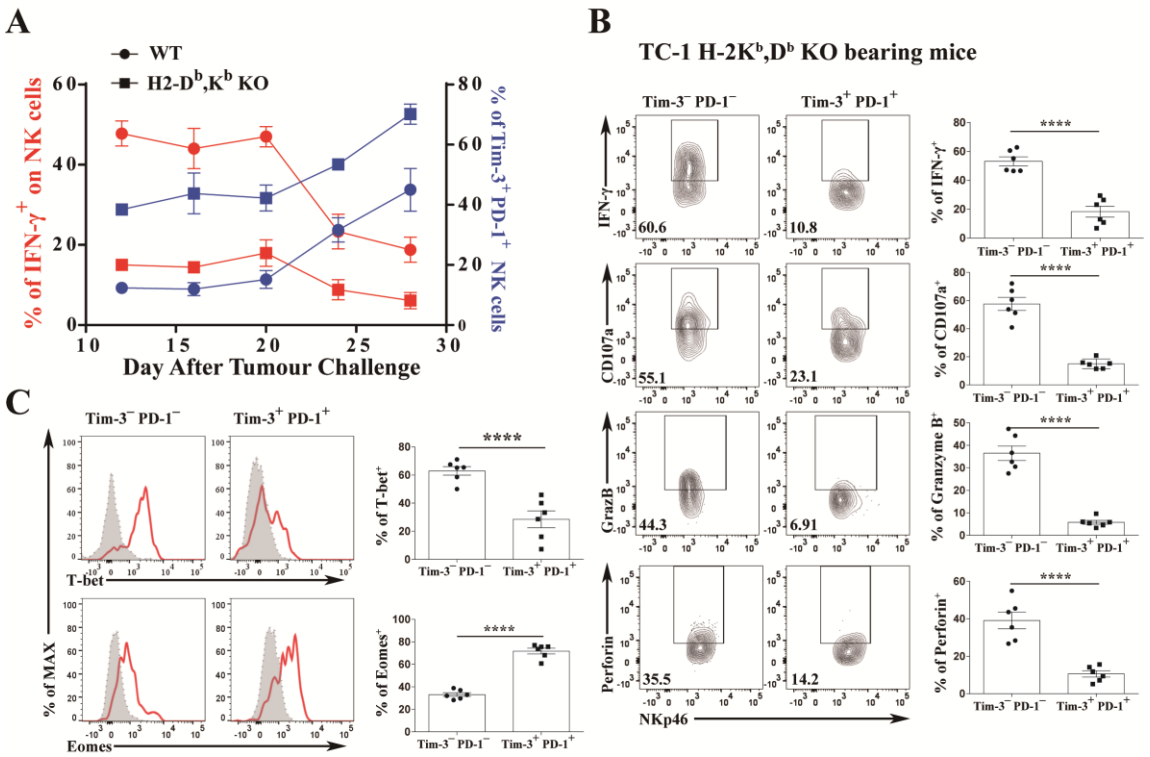

Figure 20. Infiltrating natural killer cells in MHC class I-deficient tumours are functionally exhausted. (A) The expression of Tim-3, PD-1 and IFN-γ on intratumoural NK cells from mice bearing MC38 WT or H-2K^b,D^b KO tumours was measured over time (n=5). Intratumoural NK cells were additionally restimulated with anti-NK1.1 for the analysis of IFN-γ. **(B-E)** Twelve days after TC-1 H-2K^b,D^b KO implantation, infiltrating lymphocytes were restimulated in vitro with anti-NK1.1, and the **(B)** IFN-γ, CD107a, granzyme B and perforin production, **(C)** T bet and Eomes expression were determined in Tim-3$^+$PD-1$^+$ or Tim-3$^-$PD-1$^-$ natural killer cells by flow cytometry. The data in B and C were analysed by a two-tailed unpaired Student's t test.

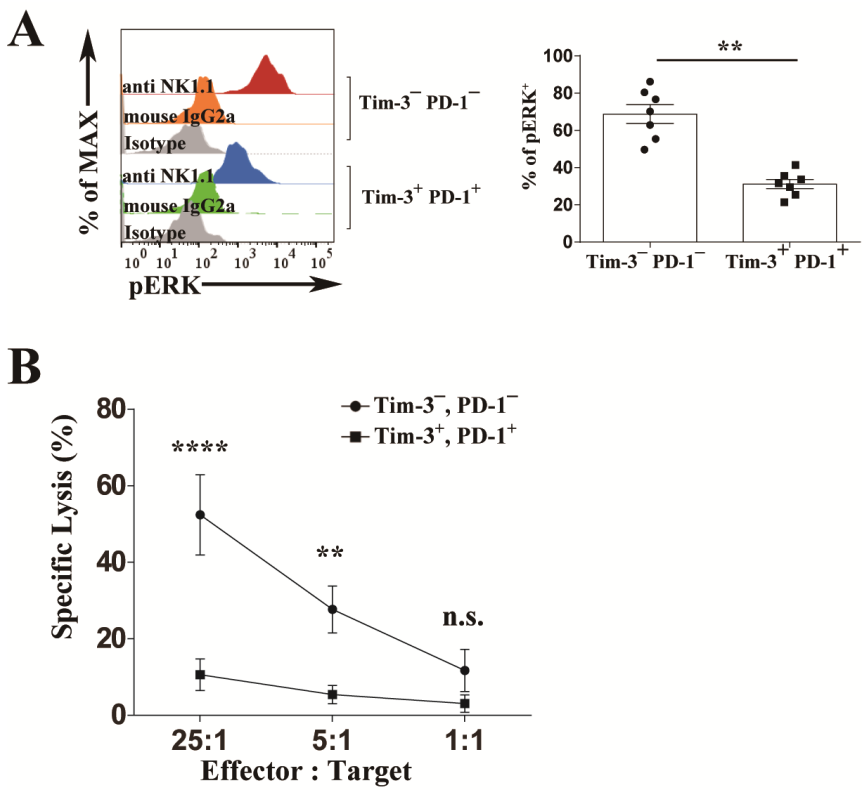

Figure 21. Infiltrating natural killer cells in MHC class I-deficient tumours are defected in ERK phosphorylation and cytotoxicity. Twelve days after TC-1 H-2K^{b},D^{b} KO implantation, infiltrating lymphocytes were restimulated in vitro with anti-NK1.1, and the **(A)** ERK phosphorylation were determined in Tim-3^{+}PD-1^{+} or Tim-3^{-}PD-1^{-} natural killer cells by flow cytometry. (**B)** Intratumoural Tim-3^{+}PD-1^{+} and Tim-3^{-} PD-1^{-} NK cells were isolated from TC-1 H-2K^{b}, D^{b} KO-bearing mice (pooled from 20 mice). They were cocultured with ^{51}Cr labelled TC-1 H-2K^{b}, D^{b} KO cells as target cells. The data in A were analysed by a two-tailed unpaired Student's t test. The data in B were analysed by a two-way ANOVA with Bonferroni multiple comparison tests *P<0.05, **P<0.01, ***P<0.001, ****P<0.0001, n.s.= not significant.

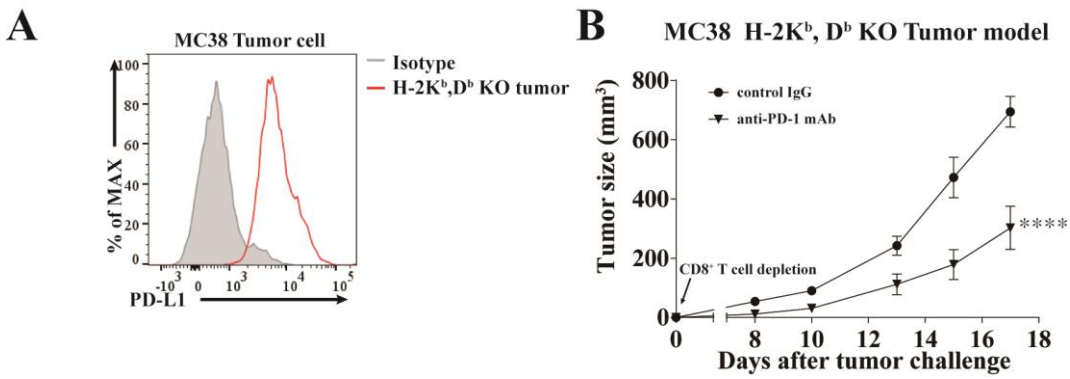

Figure 22. The PD-1/PDL1 axis transmits a negative signal on exhausted NK cells. (A) The expression level of PDL-1on MC38 H-2K^b, D^b KO was measured by flow cytometry. **(B)** MC38 H-2K^b, D^b KO tumour cells (1x10^5) were implanted into mice, which were then treated with anti-PD-1 (300 μg) or control IgG twice weekly. A depleting antibody (2.43) for CD8+ T cell depletion was injected i.p. twice weekly. The data shown are from at least 2 individual experiments with similar results. The data in B was analysed by two-way ANOVA with Bonferroni multiple comparison tests. *P<0.05, **P<0.01, ***P<0.001, ****P<0.0001.

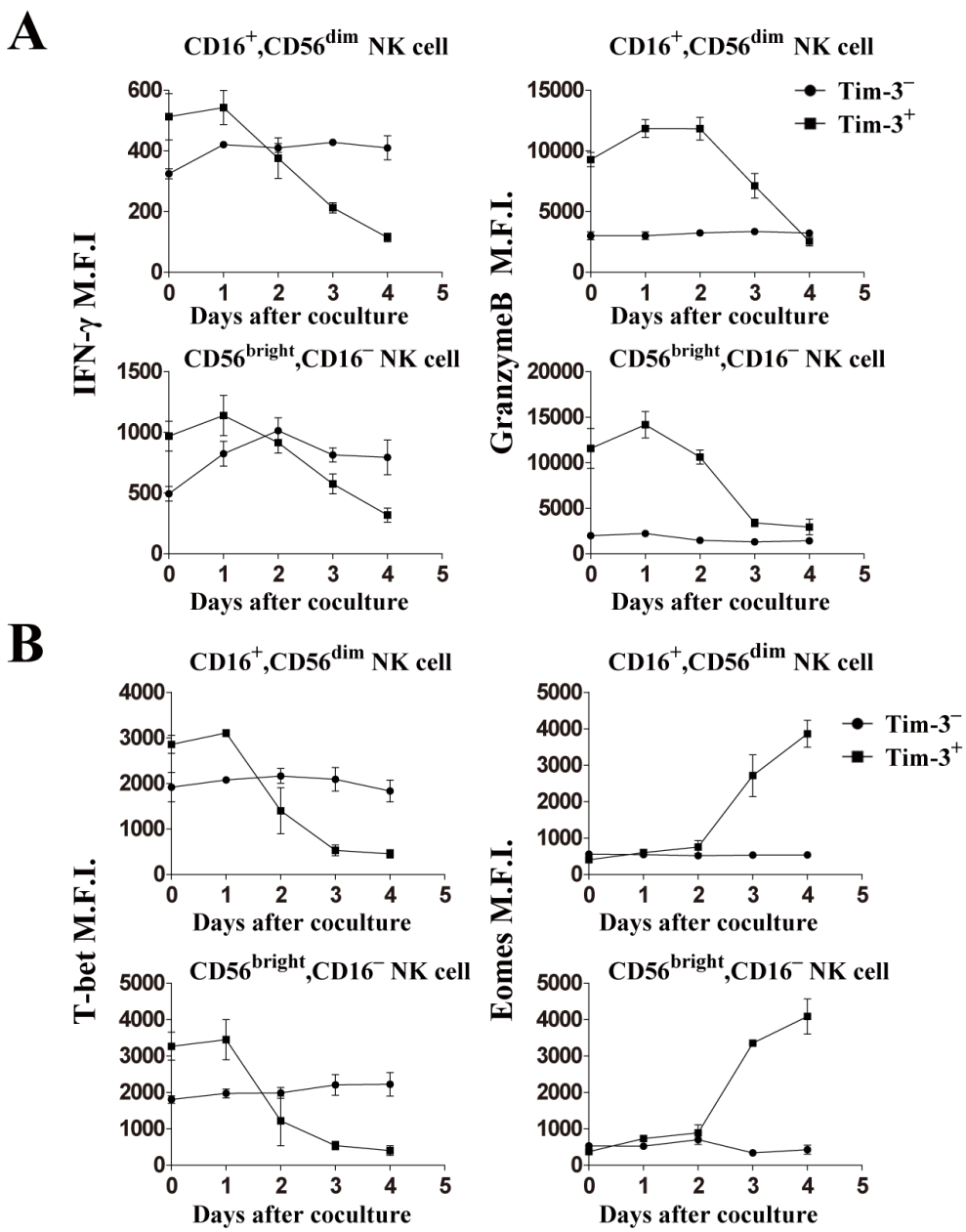

Figure 23. HeLa β2m KO cells induce dysfunction of human NK cells. **(A-B)** Tim-3$^+$ or Tim-3$^-$ human NK cells cocultured with HeLa β2m KO cells for 3 days were restimulated in vitro with human ULBP-2, and IFN-γ and granzyme B production and T-bet and Eomes expression were assessed by flow cytometry. The data shown are from at least 2 individual experiments with similar results.

IL-21 reverses the functions of exhausted NK cells

Given that vaccination with B/Mo/αGC effectively controls the growth of MHC class I-deficient tumours in an NK- and NKT cell-dependent manner, I hypothesized that the vaccination could revive the otherwise defective effector functions of NK cells in mice bearing MHC class I-deficient tumours **(Figure 11)**. Thus, I investigated whether B/Mo/αGC could reverse the exhausted status of NK cells. The frequency of IFN-γ-producing NK cells was dramatically increased with B/Mo/αGC vaccination compared with B/Mo alone, regardless of the MHC class I expression level in the tumours **(Figure 24A)**. The increase in IFN-γ-producing NK cells upon B/Mo/αGC vaccination was dependent on NKT cells because Jα281-deficient mice failed to demonstrate a similar increase **(Figure 24B)**. NKT cells are known to secrete various cytokines, including IFN-γ, IL-4, TNF-α and IL-21 [51, 52]. When B/Mo/αGC was injected, I confirmed that the NKT cells produced IFN-γ, IL4, TNF-α and IL-21 **(Figure 25)**. Therefore, I next sought to determine whether NKT cell-produced cytokines were responsible for the B/Mo/αGC-mediated recovery of NK cell functions in H-2K^b, D^b-deficient tumours. Because IL-21 and IFN-γ are well-known stimulators of NK cell functions [30, 53], I first tested whether these cytokines could revive the effector functions of exhausted NK cells in tumours. The addition of IFN-γ partially retrieved the IFN-γ-producing capacity of exhausted NK cells, whereas the addition of IL-21 completely restored the functions of NK cells isolated from H-2K^b, D^b-deficient tumours to levels comparable to those of NK cells isolated from WT tumours **(Figure 26A)**. I also found that ERK activation in NK cells was significantly increased by both IFN-γ and IL-21 in vitro **(Figure 26B)**. However, the addition of IL-4 or TNF-α did not retrieve the IFN-γ-producing capacity of exhausted NK cells **(Figure 26C)**.

To confirm the IFN-γ- and IL-21-dependent reversal of NK cell functions in vivo, I administered an anti-IFN-γ-neutralizing Ab or anti-IL-21R-blocking Ab after B/Mo/αGC vaccination. The B/Mo/αGC-mediated recovery of IFN-γ production and CD107a degranulation in Tim-3$^+$PD-1$^+$ NK

cells was significantly diminished in mice treated with the anti-IL-21R blocking Ab, while partial inhibition was observed in mice treated with the anti-IFN-γ Ab **(Figure 27)**. The recovery of T-bet expression in Tim-3^+PD-1^+ NK cells following B/Mo/αGC vaccination was also completely abrogated by IL-21R blockade **(Figure 28A)**. To address whether alterations in effector cytokine production and T-bet expression could lead to changes in the cytotoxicity exhibited by each NK cell subset, I tested the cytotoxicity of purified Tim-3^- PD-1^- and Tim-3^+PD-1^+ NK cells isolated after B/Mo/αGC vaccination. I found that B/Mo/αGC vaccination restored the cytotoxic functions of Tim-3^+PD-1^+ NK cells in MHC class I-deficient tumours and that IL-21 was required for this process because the IL-21R blockade significantly abrogated the recovery of NK cell cytotoxicity **(Figure 28B)**. Consistent with these results, the regression of H-2K^b, D^b-deficient TC-1 tumour growth following B/Mo/αGC vaccination was partially abrogated by IFN-γ neutralization, while IL-21R blockade almost completely restored tumour progression to the same extent observed in unvaccinated mice **(Figure 29A)**. This pattern was reproducible in two different MHC class I-deficient tumour models **(Figure 29B-C)**.

Next, I sought to determine whether IL-21 could directly induce the functional recovery of exhausted NK cells in MHC class I-deficient tumours. To achieve this goal, I employed Rag1$^{-/-}$ mice to eliminate the effects of IL-21 on T cells. When I intratumourally injected recombinant IL-21 (rIL-21) into MC38 H-2K^b, D^b-deficient tumour-bearing Rag 1$^{-/-}$ mice, tumour growth was significantly inhibited with an increase in tumour-infiltrating NK cells **(Figure 30A-B)**. Although the levels of Tim-3 and PD-1 expression were decreased, the expression of IFN-γ and CD107a was increased by intratumoural injection of rIL-21 **(Figure 30C-D)**. To establish and isolate fully exhausted NK cells, I used an IFN-γ-eYFP-reporter (GREAT) mouse system. I isolated Tim-3^+PD-1^+eYFP$^-$ NK cells from MC38 H-2K^b, D^b-deficient tumour-bearing GREAT mice and stimulated them with anti-NK1.1 in the presence of rIL-21. I observed that IFN-γ secretion of rIL-21-treated

Tim-3^{+}PD-1^{+}eYFP^{-} NK cells was significantly increased compared with that of vehicle-treated Tim-3^{+}PD-1^{+}eYFP^{-} NK cells **(Figure 31A)**. To analyse the direct anti-tumour effects of rIL-21-treated Tim-3^{+}PD-1^{+}eYFP^{-} NK cells, these cells were adoptively transferred into IL-2R$\gamma^{-/-}$Rag2$^{-/-}$ mice (lacking B cells, T cells and NK cells) bearing MC38 H-2K^{b},D^{b}-deficient tumours. I observed a significant inhibition of tumour growth in mice that received rIL-21-treated Tim-3^{+}PD-1^{+}eYFP^{-} NK cells. The growth inhibition in the mice that received these cells was slightly higher, although not statistically significant, than that in mice that received Tim-3^{-}PD-1^{-} NK cells **(Figure 31B).** Collectively, my results suggest that IL-21 could restore the function of exhausted Tim-3^{+}PD-1^{+} NK cells and effectively inhibit tumour progression.

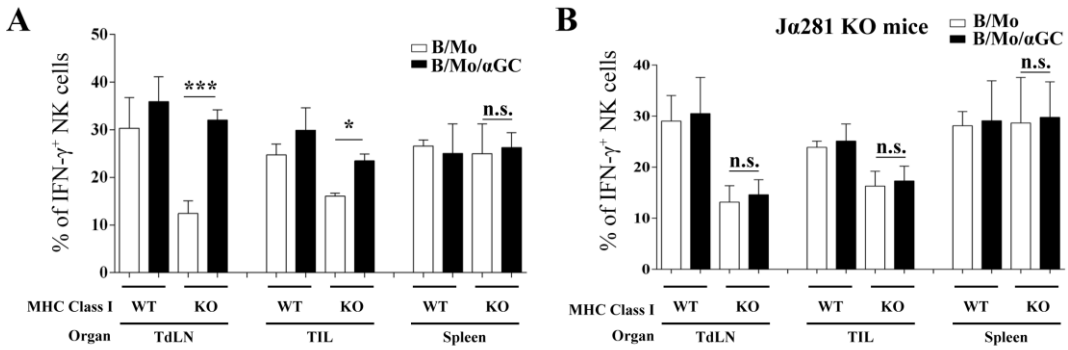

Figure 24. Exhausted NK cells induced in MHC class I knockout tumour-bearing mice are reversed by NKT-dependent activation. (A-B) Eleven days after TC-1 WT or H-2K^b,D^b KO cell implantation, each tumour-bearing **(A)** C57BL/6 or **(B)** Jα281 KO mouse was vaccinated with B/Mo or B/Mo/αGC (1x10^6). In addition, 12 hours later, lymphocytes from the indicated organs were stimulated with control IgG or anti-NK1.1 for 30 minutes, and IFN-γ production by NK cells was analysed by flow cytometry. The data were analysed using a two-tailed unpaired Student's t test. *P<0.05, **P<0.01, ***P<0.001, ****P<0.0001.

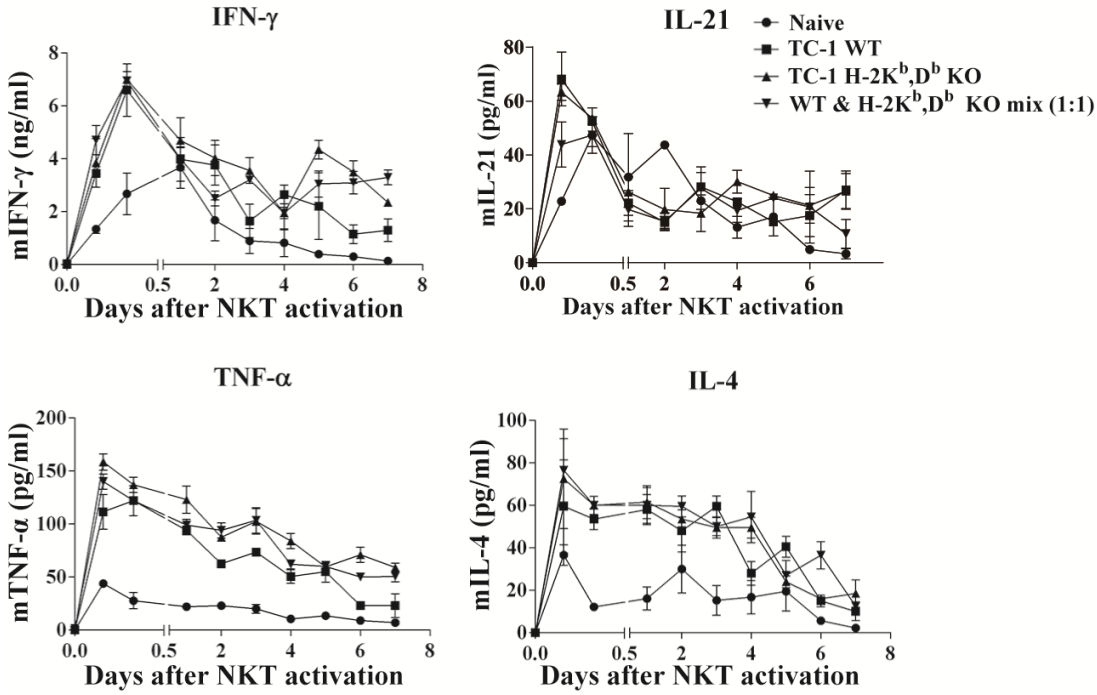

Figure 25. NKT cells induce various cytokines in tumour-bearing mice. **(A)** The cytokine profile in the serum of B/Mo/αGC-injected WT, TC-1WT, TC-1 H2-K^{b}D^b KO or WT&H-2K^b,D^b KO mixed tumour-bearing mice at various times. The levels of IL-21, IFN-γ, TNF-α and IL-4 were detected by ELISA.

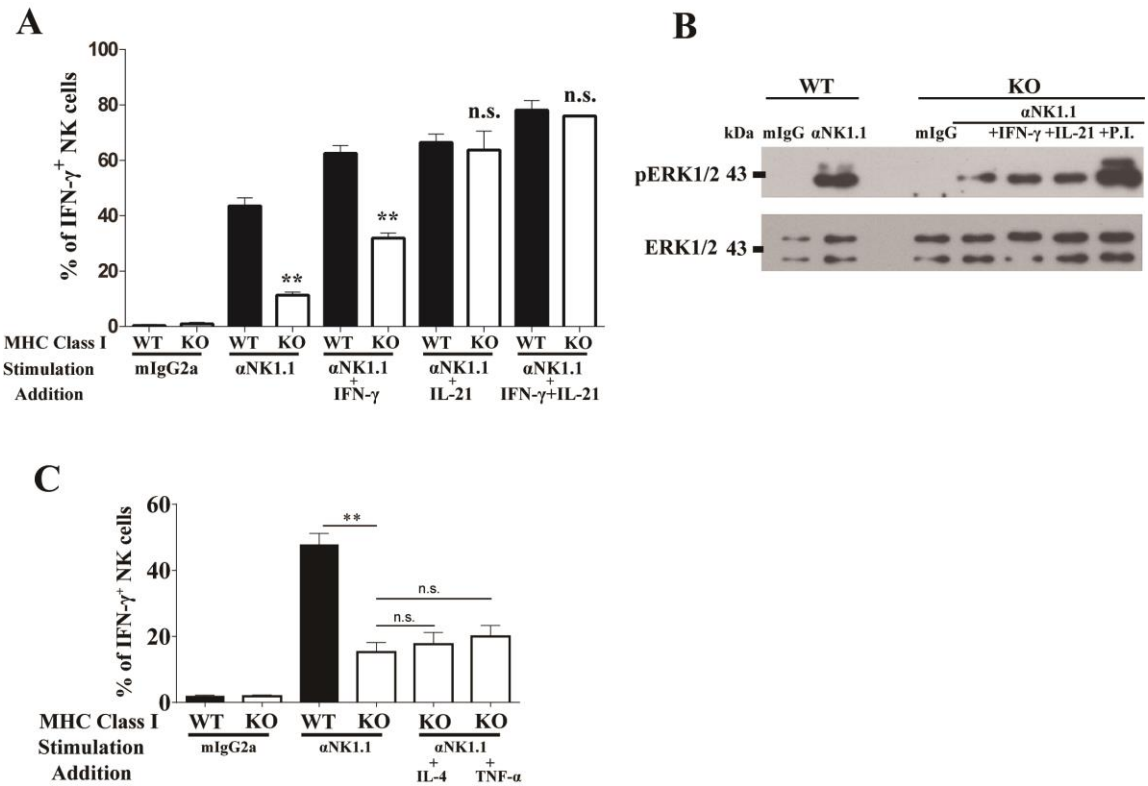

Figure 26. IL-21 mediated functional reversal of exhausted NK cell *in vitro*. Twelve days after TC-1 WT or H-2K^b,D^b KO implantation, intratumoural lymphocytes were stimulated in vitro with IFN-γ (20 ng/ml) and IL-21 (20 ng/ml) alone or in combination and after they were restimulated with anti-NK1.1. (**A)** The IFN-γ production was determined by intracellular staining, (**B)** and ERK phosphorylation was determined by western blot analysis. (**(C)** Twelve days after TC-1 WT or H-2K^b,D^b KO implantation, intratumoural lymphocytes were stimulated in vitro with TNF-α (20 ng/ml) and IL-4 (20 ng/ml) and then restimulated with anti-NK1.1. The data were analysed using a two-tailed unpaired Student's t test. *P<0.05, **P<0.01, ***P<0.001, ****P<0.0001.

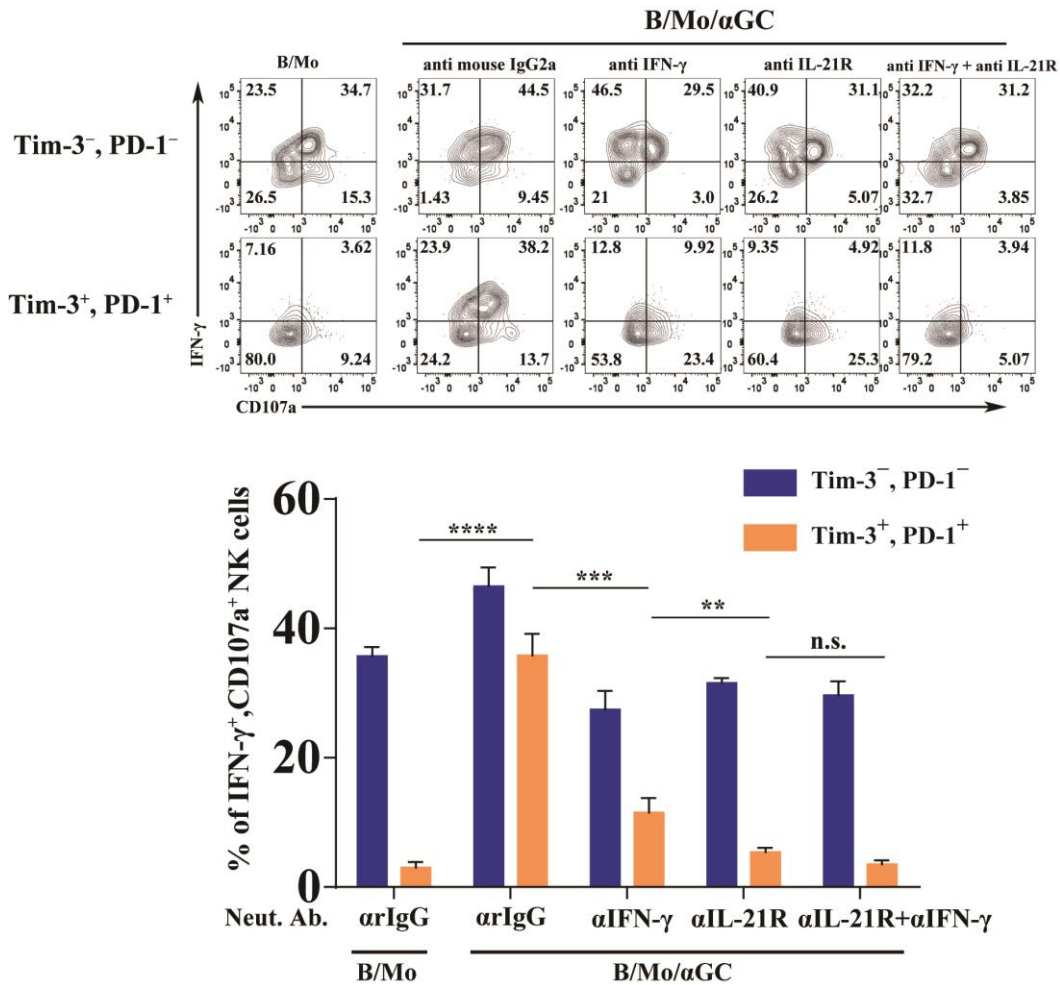

Figure 27. IL-21-dependent functional (IFN-γ secretion and CD107a degranulation) reversal of Tim-3$^+$ PD-1$^+$ natural killer cells *in vivo*. Nine days after TC-1 H-2K^b,D^b KO implantation, anti-IFN-γ (500 μg/mouse) or anti-IL-21R (300 μg/mouse) or both were injected via i.p. and two days later, B/Mo/αGC (1x10^6 cells/mouse) was injected along with the neutralizing antibodies. In addition, 12 hours later, infiltrating lymphocyte were restimulated in vitro with anti-NK1.1 and IFN- γ, CD107a were assessed by flow cytometry.

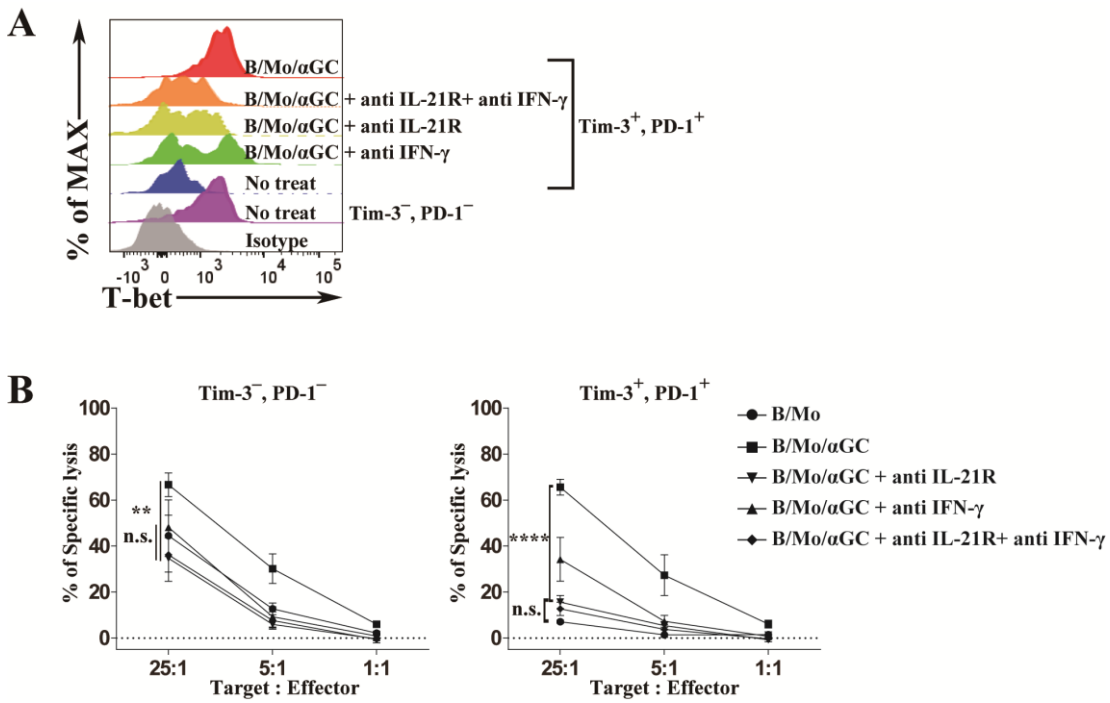

Figure 28. IL-21-dependent functional (T-bet expression and cytotoxicity) reversal of Tim-3$^+$ PD-1$^+$ natural killer cells *in vivo*. Nine days after TC-1 H-2K^b,D^b KO implantation, anti-IFN-γ (500 μg/mouse) or anti-IL-21R (300 μg/mouse) or both were injected via i.p. and two days later, B/Mo/αGC (1x10^6 cells/mouse) was injected along with the neutralizing antibodies. In addition, 12 hours later, (**A-B)** infiltrating lymphocyte were restimulated in vitro with anti-NK1.1 and (**A**) T-bet expression were assessed by flow cytometry. (**B)** Infiltrating Tim-3$^+$PD-1$^+$ and Tim-3$^-$PD-1$^-$ natural killer cell were isolated in TC-1 H-2K^b,D^b KO bearing mice (pooled from 20 mice). They were cocultured with ^{51}Cr labelled TC-1 H-2K^b, D^b KO.

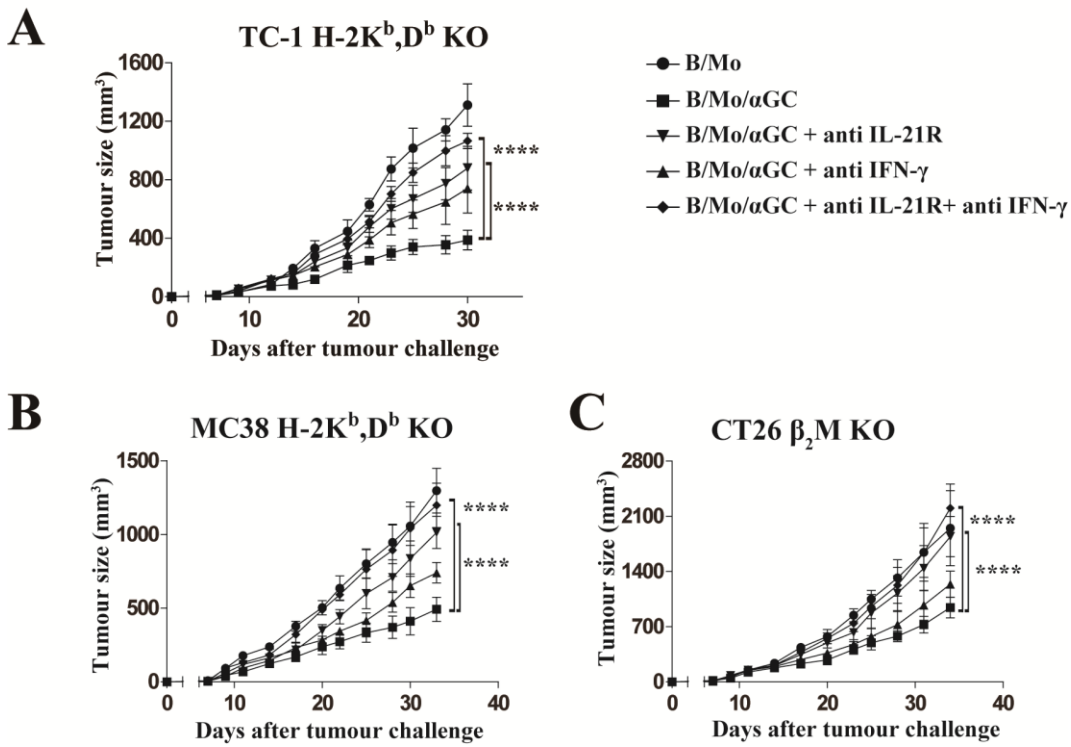

Figure 29. Figure 15. IL-21-dependent functional reversal (anti-tumour effects) of exhausted Tim-3$^+$ PD-1$^+$ natural killer cells. (A-C) Subcutaneous growth of TC-1 **(A)**, MC38 **(B)** and CT26 **(C)** WT and MHC Class I KO tumour cells in each mice (n=6) treat with B/Mo(1x10^6), B/Mo/αGC(1x10^6) every week with indicated neutralizing antibodies.

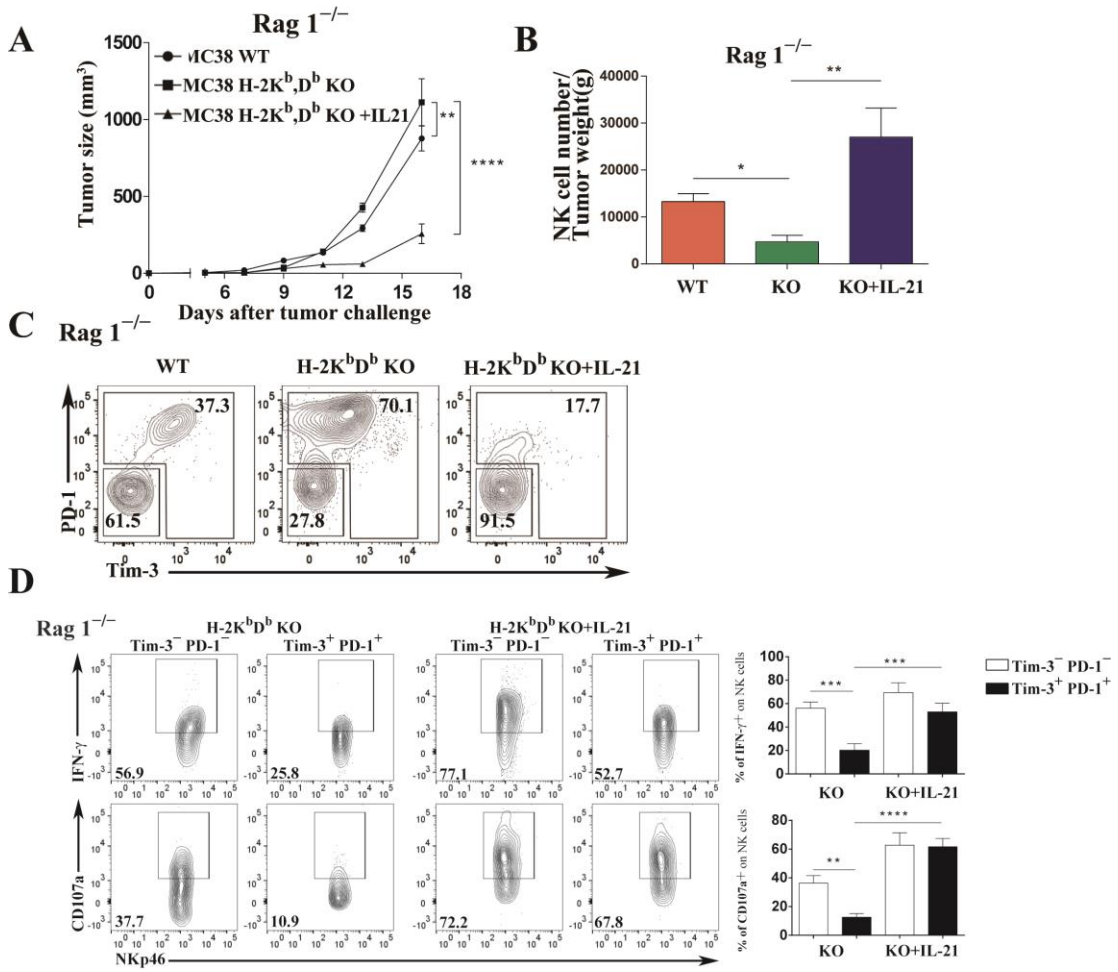

Figure 30. Intratumoural injection of IL-21 induces functional reversal of exhausted Tim-3$^+$ PD-1$^+$ NK cells in Rag$^{-/-}$ mice. (A-E) MC38 WT- or H-2K^b,D^b KO-bearing Rag 1$^{-/-}$ mice (n=5) were treated with IL-21 (10 μg/mouse) by intratumoural injection every 3 days from days 9 to 15. **(A)** Tumour growth was measured using a metric calliper 2-3 times per week. (**B)** The number of NK cells was analysed as $(= \frac{\%\text{ of CD45.2 NKp46 cells x No.of tumor infiltrating lymphocyte}}{Tumor\ weight\ (g)})$. **(C-D)** Tumour-infiltrating lymphocytes were restimulated using anti-NK1.1, and **(C)** the expression of Tim-3 and PD-1 and **(D-E)** the production of IFN-γ and CD107a were analysed in the indicated cell populations.

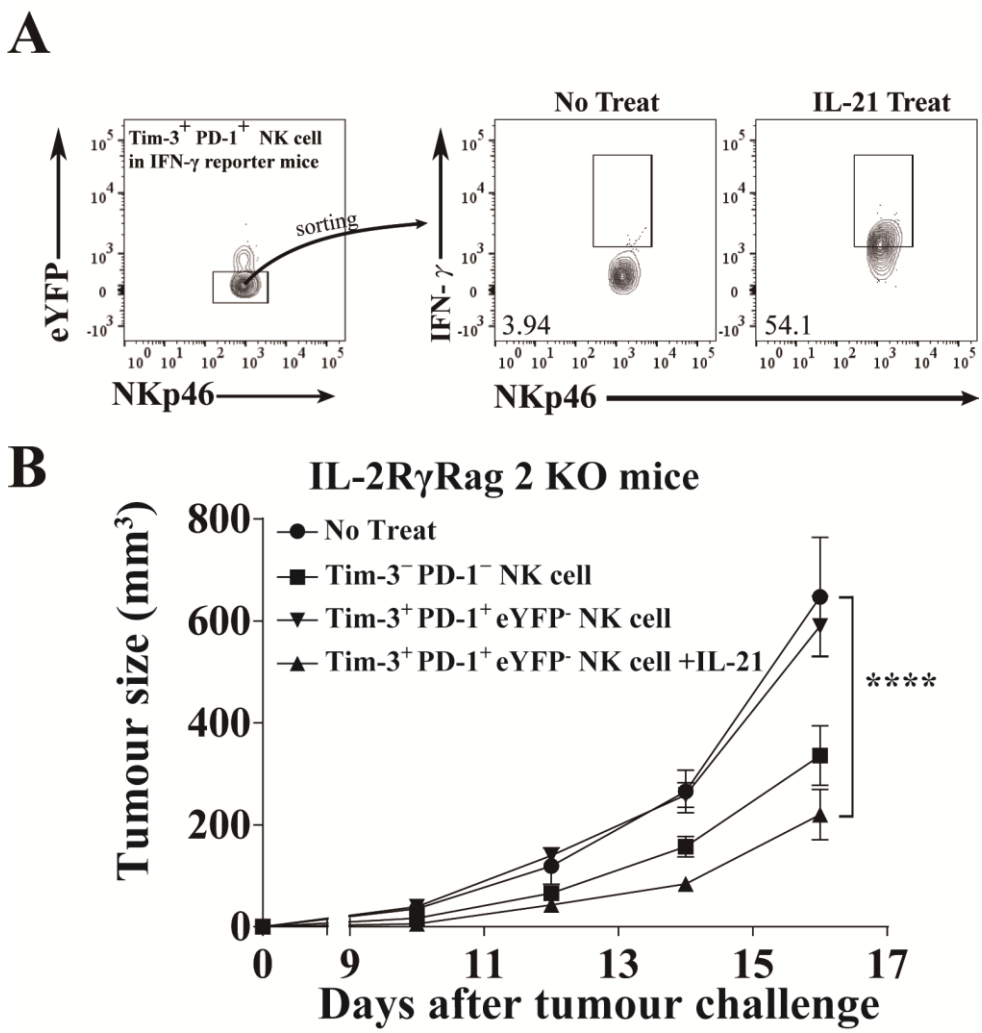

Figure 31. IL-21 directly induce functional reversal of fully exhausted Tim-3$^+$ PD-1$^+$ natural killer cells in GREAT mice *in vivo*.

(A) IFN-γ-eYFP-reporter (GREAT) mice were implanted with MC38 H-2K^b,D^b KO tumour cells and intratumoural Tim-3$^+$ PD-1$^+$eYFP$^-$ NK cells were sorted and incubated overnight in the presence or absence IL-21 (20 ng/ml) with anti-NK1.1 stimulation last 5 h. IFN-γ secretion was analysed by flow cytometry. **(B)** Tumour growth in IL-2Rγ$^{-/-}$Rag2$^{-/-}$ mice that received the indicated group of cells (1 × 10^5) (n = 10). MC38 H-2K^b, D^b-deficient tumour cells (5× 10^4) were inoculated 1 day before NK cell transfer.

IL-21 mediated mechanism of reversal of exhausted NK cells

To further explore the underlying signalling mechanisms of IL-21-mediated functional reversal of exhausted Tim-3^{+}PD-1^{+} NK cells, I examined the ERK/MAPK, PI3K-AKT and STAT pathways because IL-21 has been suggested to be transduced via these signalling pathways [30]. I found that IL-21 induced ERK, AKT, STAT1 and STAT3 phosphorylation **(Figure 26B, 32A, 32C and 32E)**. When exhausted Tim-3^{+}PD-1^{+} NK cells were pretreated with various signalling inhibitors, IFN-γ secretion and T-bet upregulation by IL-21 were reduced in a dose-dependent manner by Fludarabine (STAT1 inhibitor) and LY294002 (PI3K inhibitor) **(Figure 32B, 32F and 32G)**. However, PD98059 (ERK inhibitor) and S31-201 (STAT3 inhibitor) did not reduce IFN-γ secretion **(data not shown, Figure 32D)**. I also analysed the Foxo1 and T-bet transcription factors. The PI3K-AKT pathway is known to enhance proliferation [41] and upregulate T-bet via Foxo1 phosphorylation [42]. The Foxo1 transcription factor negatively regulates the effector functions of NK cells by inhibiting T-bet expression [54]. I found that intratumoural rIL-21 treatment elicited Foxo1 phosphorylation and T-bet upregulation in NK cells **(Figure 33A)**. I also confirmed that the addition of exogenous rIL-21 induced Foxo1 phosphorylation in exhausted human NK cells **(Figure 33B)**. Collectively, these results suggest that STAT1 and the PI3K-AKT-Foxo1 axis are crucial regulators of the IL-21-mediated reversal of exhausted Tim-3^{+}PD-1^{+} NK cells.

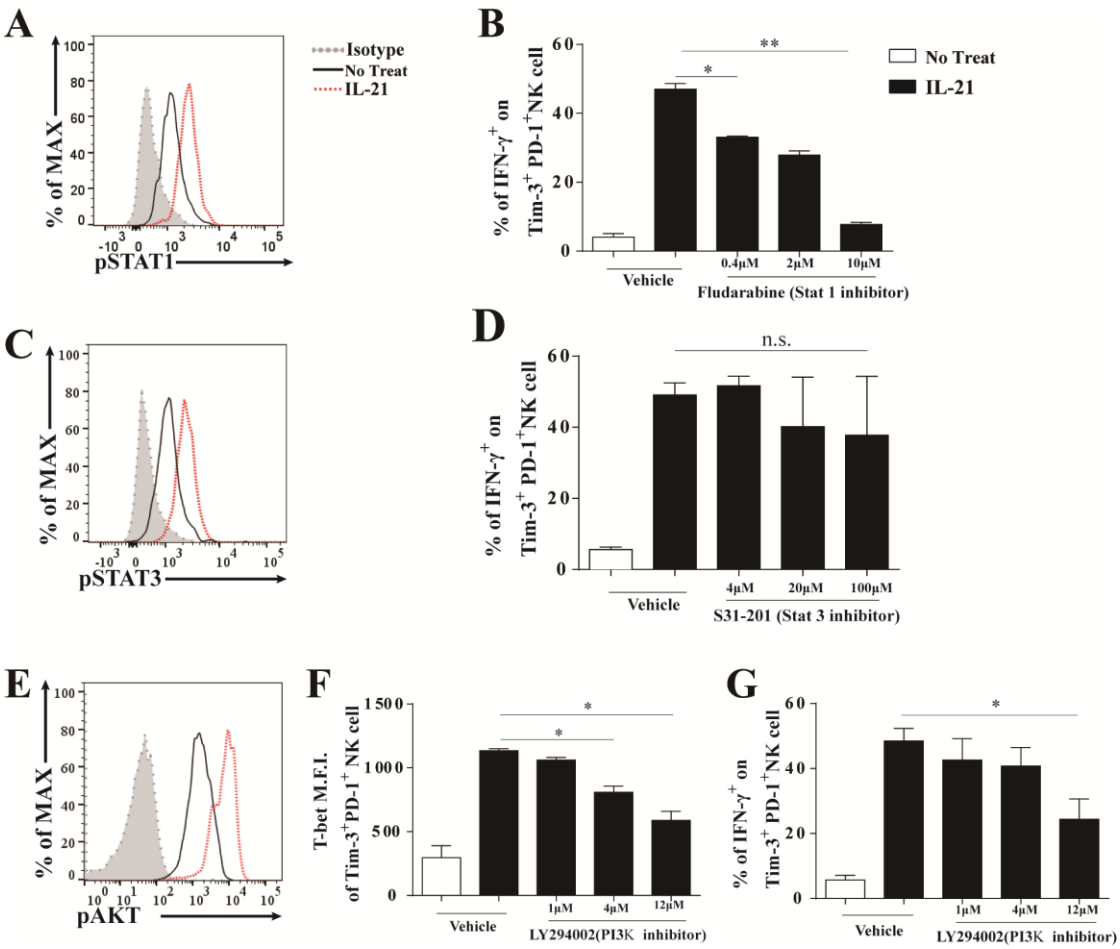

Figure 32. STAT1 and the PI3K-AKT pathway are associated with the IL-21-mediated functional reversal of Tim-3$^+$PD-1$^+$ NK cells. The expression of phospho-STAT1 **(A)**, phospho-STAT3 **(C)**, and phospho-AKT **(E)** on Tim-3$^+$PD-1$^+$ NK cells was analysed after a 1-h incubation with or without rIL-21 (20 ng/ml). IFN-γ (**B**, **D** and **G**) and T-bet (**F**) expression on Tim-3$^+$PD-1$^+$ NK cells treated with either vehicle (DMSO) or indicated concentrations of Fludarabine (STAT1 inhibitor) **(B)**, S31-201 (STAT3 inhibitor) **(D)** or LY294002 (PI3K inhibitor) **(F-G)** for 30 min, followed by overnight incubation in the presence or absence of rIL-21 (20 ng/ml) and stimulation with anti-NK1.1.

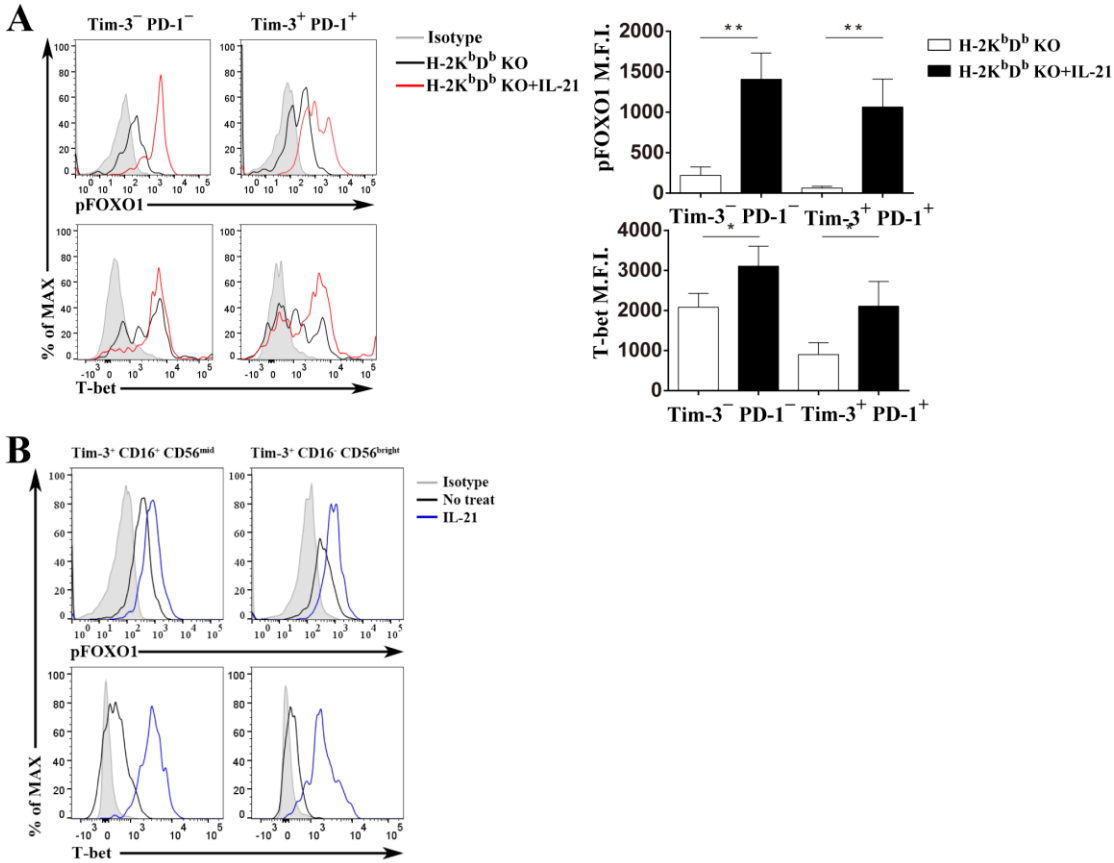

Figure 33. IL-21 elicits Foxo1 phosphorylation and T-bet upregulation in mice and humans. (A) Intracellular staining of pFOXO1 and T-bet in Tim-3^{+}PD-1^{+} and Tim-3^{-}PD-1^{-} NK cells from MC38 H-2K^{b},D^{b} KO-bearing Rag 1$^{-/-}$ mice that were treated with IL-21 (10 μg/mouse) by intratumoural injection every 3 days. (B) Intracellular staining of pFOXO1 and T-bet in the indicated NK cells stimulated with IL-21 (50 ng/ml) in vitro for 1 hour. The data were analysed using a two-tailed unpaired Student's t test. *P<0.05, **P<0.01, ***P<0.001.

Reversal of exhausted NK cells in cancer patients by IL-21

Recently, PD-1^+ and Tim-3^+ NK cells were identified in the tumour tissues of cancer patients [25, 55, 56]. However, the characteristics of these intratumoural NK cells in cancer patients have not yet been fully investigated. To confirm the presence of Tim-3^+PD-1^+ NK cells in cancer patients, I analysed tumour tissues isolated from patients with different types of cancer. When I isolated NK cells from human tumour tissues based on CD16 and CD56 coexpression, the expression levels of Tim-3 and PD-1 on intratumoural NK cells were much higher than those in normal tissues of the same patients **(Figure 34A, 34C)**. MHC class I expression in $EpCam^+$ tumour tissues was lower than that in $EpCam^+$ normal tissues **(Figure 34B)**, suggesting that Tim-3 and PD-1 expression on intratumoural NK cells was presumably induced by MHC class I downregulation in the tumour tissues of cancer patients.

Functional analysis revealed that the effector function of intratumoural Tim-3^+PD-1^+ NK cells was defective as follows: the secretion of IFN-γ and granzyme B and the cytotoxicity of the Tim-3^+PD-1^+ NK cells were significantly reduced compared with those of the Tim-3^-PD-1^- counterparts. Intriguingly, however, rIL-21 treatment restored IFN-γ and granzyme B secretion and the cytotoxicity of Tim-3^+PD-1^+ NK cells to levels comparable to those of Tim-3^-PD-1^- NK cells **(Figure 35A, 35B and 36)**. Taken together, these results suggest that the functional exhaustion of Tim-3^+PD-1^+ NK cells in the tumour tissues of cancer patients can be restored by exogenous IL-21 treatment.

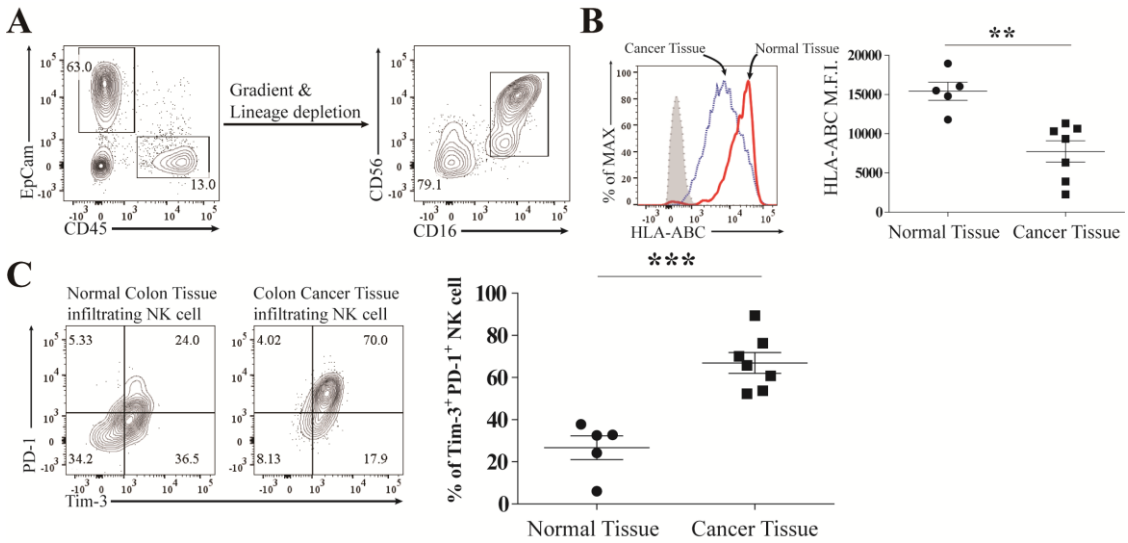

Figure 34. Expression level of Tim-3 and PD-1 on intratumoural NK cells in cancer patients (A) The expression of EpCam and CD45 in the primary tumour tissues or normal tissues was analysed by flow cytometry. Intratumoural NK cells were isolated by gradient centrifugation, followed by depletion of lineage (EpCam, CD3, CD19, CD14)$^{+}$ cells. **(B)** HLA-ABC expression on gated EpCam^{+} tumour or normal tissues from cancer patients. **(C)** Tim-3 and PD-1 expression on gated CD16^{+}CD56^{+} intratumoural NK cells from cancer patients.

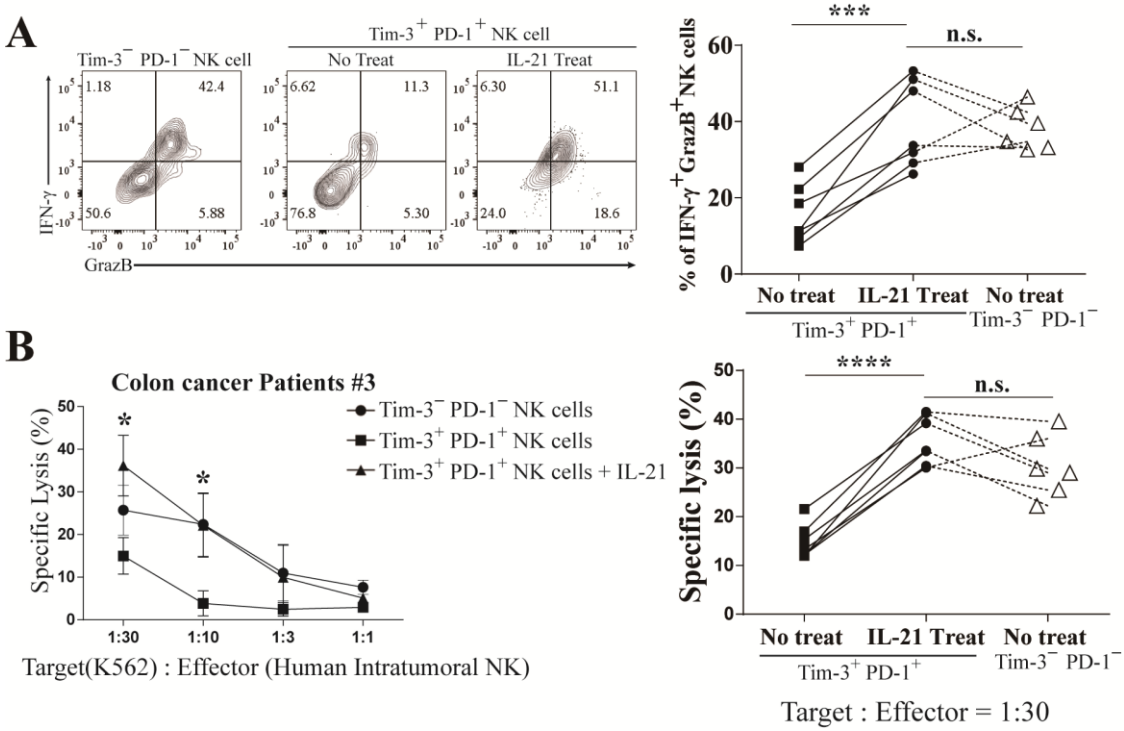

Figure 35. Rescue of exhausted Tim-3⁺ PD-1⁺ NK cells by IL-21 in cancer patients. (A) Isolated Tim-3⁺PD-1⁺ or Tim-3⁻PD-1⁻ NK cells were incubated overnight in the presence or absence of rIL-21 (20 ng/ml) and stimulated with anti-hNKp46 for 5 h. The IFN-γ and granzyme B expression on the indicated cells is depicted. **(B)** Isolated Tim-3⁺PD-1⁺ or Tim-3⁻PD-1⁻ NK cells were incubated overnight in the presence or absence of rIL-21 (20 ng/ml) and were cocultured with ^{51}Cr-labeled K562 cells as target cells. The data were analysed by a two-tailed unpaired Student's t test *P<0.05, **P<0.01, ***P<0.001, ****P<0.0001. The data are cumulative from five (normal tissue) or seven (tumour tissue) independent experiments. All values represent the mean ± s.e.m.

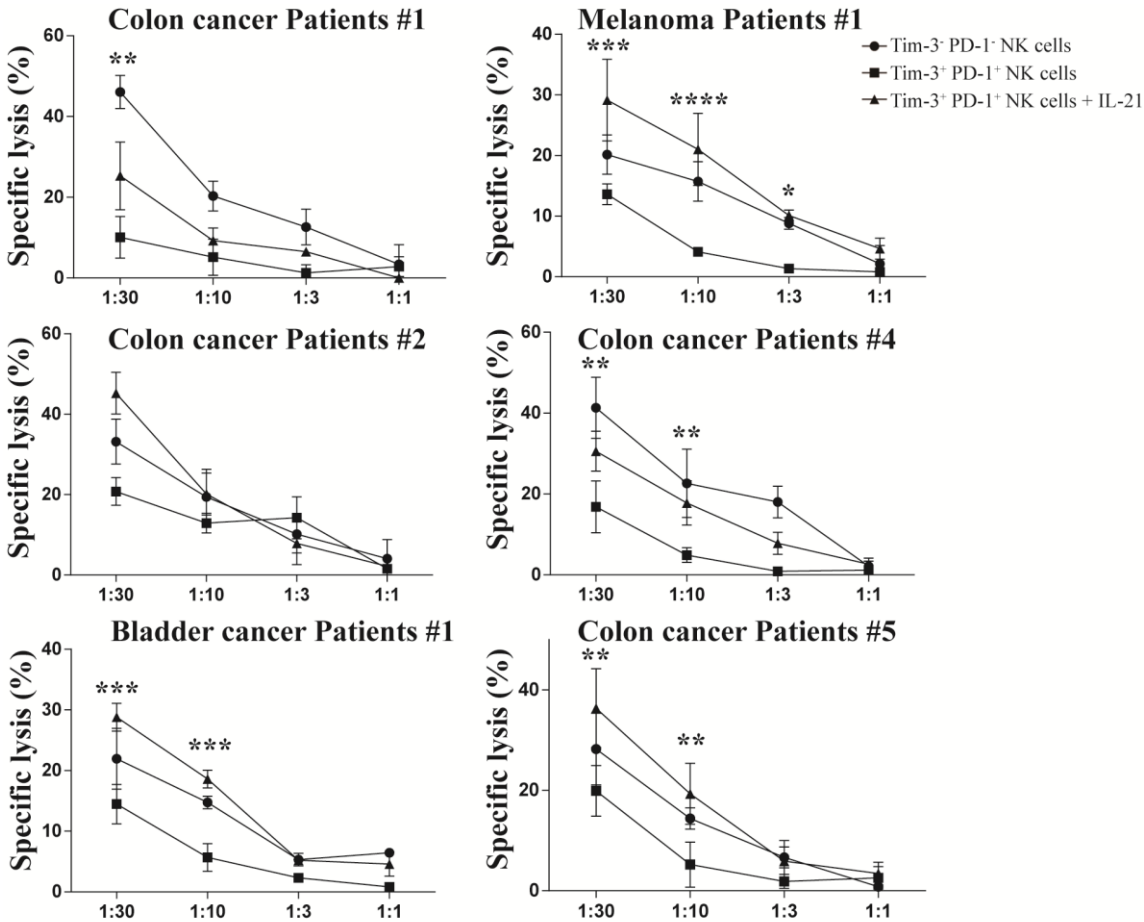

Figure 36. *In vitro* cytotoxicity of intratumoural NK cells from cancer patients. Isolated Tim-3^{+}PD-1^{+} or Tim-3^{-}PD-1^{-} NK cells were incubated overnight in the presence or absence of rIL-21 (20 ng/ml) and cocultured with ^{51}Cr-labeled K562 cells as target cells. The data were analysed by two-way ANOVA with Bonferroni multiple comparisons tests. *P<0.05, **P<0.01, ***P<0.001, ****P<0.0001

Antibody	Clone	Dilution	Manufacturer	Cat#
H-2Db	KH95	1:100	Biolegend	1115
H-2Kb	AF6-88.5	1:100		1165
PD-1	RMP1-14	1:100		1141
PDL-1	10F.9G2	1:100		1243
Tim-3	RMT3-23	1:50		1197
CD3ε	145-2C11	1:100		1003
CD19	6D5	1:100		1155
Gr-1	RB6-8c5	1:100		1084
TER-119	TER-119	1:100		1162
NKp46	29A1.4	1:50		1376
NK1.1	PK136	1:50		1087
CD45.2	104	1:100		1098
CD45	2D1	1:100		3685
CD45	HI30	1:100		3040
CD11b	M1/70	1:100		1012
CD27	LG.3A10	1:100		1242
Ly49A	YE1/48.10.6	1:100		1168
Ly49D	4E5	1:100		1383
CD226	10E5	1:100		1288
CD69	H1.2F3	1:100		1045
CD150	A12	1:100		3063
TIGIT	1G9	1:100		1421
CD226	11A8	1:100		3383
2B4	m2b4(B6)458.1	1:100		1335
CD49b	DX5	1:100		1089
EpCam	9C4	1:100		3242
p44/42 MAPK (Erk1/2)	137F5	1:1000	Cell Signaling	4695
Phospho-p44/42 MAPK (Erk1/2) (Thr202/Tyr204)	197G2	1:1000		4377
Phospho-FoxO1 (Ser256)		1:100		9461

Antibody	Clone	Dilution	Manufacturer	Cat#
NKG2A/C/E	20d5	1:100	ebioscience	5896
PD-1	J43	1:100		9985
KLRG1	2F1	1:100		5893
2B4	eBio244F4	1:100		2441
IFN-γ	XMG1.2	1:50		7311
CD107a	eBio1D4B	1:100		1071
Granzyme B	NGZB	1:50		8898
Perforin	eBioOMAK	1:50		9392
T-bet	eBio4B10	1:100		5825
Ly49A/D	12A8	1:100		5783
Eomes	Dan11mag	1:100		4875
NKG2D	1D11	1:100		5878
CD69	FN50	1:100		0699
CD160	BY55	1:100		1609
HLA-ABC	W6/32	1:100		9983
PD-1	MIH4	1:100		9969
Tim-3	F38-2E2	1:100		3109
TIGIT	MBSA43	1:100		9500
KLRG1	13F12F2	1:100		9488
IFN-γ	4S.B3	1:50		7319
Granzyme B	GB11	1:50		8899
Eomes	WD1928	1:100		4877
Fixable Viablility Dye		1:1000		65-0865
pAKT(pT308)	J1-223.371	1:50	BD bioscience	558275
pSTAT1(pY701)	4a	1:50		562069
pSTAT3(pS727)	4/P-STAT3	1:50		562072
pERK1/2(pT202/pY204)	20A	1:50		561992
mouse CD1d PBS-57 tetramer		1:5000	NIH Tetramer core facility	

Table 1. Antibody information for flow cytometry and western blot.

Discussion

To date, MHC class I downregulation or deficiency has been reported in the tumour microenvironment of patients with various advanced cancers [2, 9, 11]. The tolerogenic tumour microenvironment induced by MHC class I insufficiency in tumour cells is one of the major impediments to effective cancer immunotherapy due to the restriction of the cytotoxicity of T lymphocytes and the induction of NK cell dysfunction [5]. Thus, it remains an unsolved question whether the concomitant activation of both adaptive and innate immune responses by immunotherapies is sufficient to overcome the tolerogenic tumour microenvironment found in advanced cancers containing MHC class I-deficient cells. Here, I demonstrate that both the induction of adaptive immune responses and the reversal of NK cell exhaustion are critical for the treatment of late-stage cancers.

Previous studies have demonstrated that the activation of NK cells is regulated by the integration of signals derived from activation and inhibitory receptors expressed on their surface [6]. For example, triggering inhibitory receptors on NK cells by the ligation of MHC class I expressed on target cells interferes with cytotoxicity-promoting signals from activating receptors, resulting in the inhibition of target cell lysis by NK cells [7]. In contrast, the downregulation of MHC class I on target cells releases NK cells from inhibitory signals to induce target cell lysis [8]. Paradoxically, MHC class I deficiency in advanced human cancers has been associated with NK cell hyporesponsiveness, which suggests that MHC class I-deficient tumour cells have evolved to escape immunosurveillance by NK cells through previously unrecognized effects on NK cells [4, 5, 9, 25]. In this regard, my findings provide direct evidence to explain why NK cells in cancer patients are unable to kill MHC class I-deficient or low-expressing tumour cells.

Tim-3 and PD-1 have recently emerged as specific markers for T cell exhaustion during chronic viral infection and cancer progression [13, 14]. Although the functional exhaustion of NK cells has also been demonstrated

in both tumour-bearing mice and cancer patients, cell surface markers that can identify exhausted NK cells in the cancer microenvironment remain unclear [24, 55]. Here, I found that the co-inhibitory receptors Tim-3 and PD-1 marked functionally defective cells among tumour-infiltrating NK cells in mice and humans alike and that tumour cells, especially MHC class I-deficient tumour cells, directly induced Tim-3^{+}PD-1^{+} NK cells. I hypothesized that perhaps, similar to T cell studies in which multiple rounds of TCR stimulation induce PD-1 in chronic viral infection, chronic interaction with MHC class I-deficient tumours induces these markers on NK cells. In addition, the degranulation, cytokine secretion and cytotoxicity of Tim-3^{+}PD-1^{+} NK cells were more defective than those of Tim-3^{-}PD-1^{-} NK cells. My study also showed that the expression levels of Tim-3 and PD-1 on intratumoural NK cells from patients with different types of cancer were much higher than those in normal tissues of the same patients. I also found that the expression of Tim-3 and PD-1 on intratumoural NK cells was inversely correlated with MHC class I expression in the tissues of cancer patients. Although previous studies have demonstrated that PD-1 and Tim-3 expression on NK cells from cytomegalovirus-infected or cancer patients transmits negative signals on NK cell cytotoxicity [22, 24, 25, 55], a few unknown features remain to be elucidated regarding the induction of the functional exhaustion of NK cells, including (i) whether the ligation of PD-1/PD-L1 or Tim-3/galactin-9 on NK cells is required for the induction of NK cell exhaustion, (ii) the molecular mechanism by which NK cell exhaustion is induced by tumour cells and (iii) the molecular mechanisms involved in the upregulation of PD-1 and Tim-3 on NK cells. For example, it has been demonstrated that Tim-3 or PD-1 ligation on T cells inhibits TCR stimulation-dependent signalling pathways and promotes exhaustion of $CD8^{+}$ T cells through the induction of NFAT [57]. Therefore, further studies are needed to identify the precise mechanism by which PD-1 and Tim-3 signalling influence the dysfunction of NK cells and to address which molecular

machineries are involved in the induction of NK cell exhaustion during cancer progression.

Previous studies have demonstrated that the production of IFN-γ by NK cells increases in a STAT1-dependent manner [58, 59], whereas the cytotoxicity of NK cells is abrogated through the STAT3 pathway [60], suggesting that STAT1 and STAT3 can oppose each other in the regulation of NK cells. In addition, the MAPK/ERK and PI3K/AKT pathways are important for promoting cytokine secretion and proliferation by NK cells [61, 62]. My results suggest that IL-21 treatment induces STAT1, STAT3, ERK and AKT phosphorylation. However, the functional reversal of exhausted NK cells appears to be mediated by STAT1 and the PI3K-AKT-Foxo1 pathway. These two mechanisms may act synergistically to promote the functional reversal of NK cell exhaustion.

Prior studies have demonstrated that neo-antigens or various antigens targeted by cancer immunotherapeutic vaccines are important for inducing anti-tumour effects [63, 64, 65] and that combination therapy (checkpoint blockade, cancer vaccines, cytokines and antibodies) with the induction of adaptive and innate immune responses could eradicate large established tumours in experimental mice [66]. In agreement with these findings, my data suggest that the spontaneous downregulation of MHC class I on tumour cells contributes to tumour evasion from immunosurveillance; to our knowledge, these advanced tumours have not previously been curable by a single immunotherapy relying on endogenous immune responses, but IL-21 secretion by NKT cell-activating vaccination or IL-21-mediated NK cell therapies effectively eradicate these tumours by reversing NK cell exhaustion. I suggest that not only inducing antigen-specific T cell and innate immune responses but also restoring NK cell exhaustion via IL-21 signalling are crucial for overcoming cancer immuno-evasion. It may be important for eliminating heterogeneous tumours containing MHC class I-deficient cells, which induce NK cell exhaustion. In addition, the provision of exogenous IL-21 may expand antigen-specific $CD8^+$ T cells and limit $CD8^+$ T cell

exhaustion [32, 33, 34, 40]. In this regard, future studies should explore whether our vaccine could also restore the exhaustion of $CD8^+$ T cells in tumour microenvironments through IL-21 produced by the activated NKT cells.

To my knowledge, this is the first report to define Tim-3^+PD-1^+ NK cells as exhausted cells induced by MHC class I-deficient tumours in mice and humans. In addition, my study explains how MHC class I-deficient tumours escape cancer immunosurveillance, despite their increased susceptibility to NK cell-mediated cell cytotoxicity during the initial stage. Furthermore, I clearly demonstrated that IL-21 can reverse the functional exhaustion of NK cells by activating both the PI3K-AKT-Foxo1 and STAT1 signalling pathways. Therefore, these findings demonstrate that NK cell exhaustion is an attractive drug target for developing anticancer immunotherapies and show that enhancing the concentration of IL-21 in the tumour microenvironment can be highly beneficial for the treatment of advanced tumours enriched with dysfunctional NK cells.

Summary

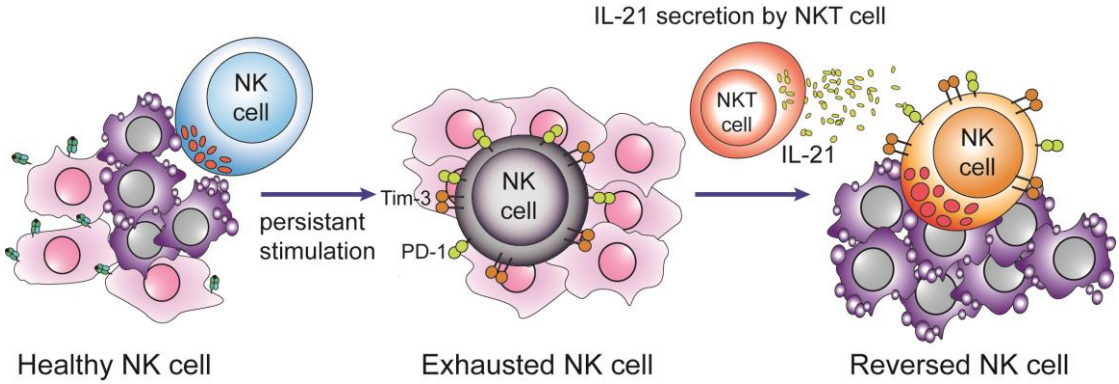

Figure 37. Cartoon summary of this study: IL-21 mediated reversal of exhausted natural killer cell facilitates anti-tumour immunity in MHC class I deficient tumours.

In this study, I showed that MHC class I-deficient tumor cells directly induced the functional exhaustion of mouse & human Tim-3^{+}PD-1^{+} NK cell population. Using various in vitro and in vivo systems, I convincingly demonstrated that the effector functions of Tim-3^{+}PD-1^{+} NK cells, such as cytokine secretion and cytotoxicity, are significantly reduced compare to Tim3^{-}PD-1^{-} counterparts in tumor bearing mice and cancer patients. Importantly, I also found that IL-21 could restores the exhausted effector functions through PI3K-AKT-Foxo1 and STAT1 dependent manner.

References

1. Zou W, Wolchok JD, Chen L. PD-L1 (B7-H1) and PD-1 pathway blockade for cancer therapy: Mechanisms, response biomarkers, and combinations. *Science translational medicine* **8**, 328rv324-328rv324 (2016).

2. Turcotte S, *et al.* Phenotype and function of T cells infiltrating visceral metastases from gastrointestinal cancers and melanoma: implications for adoptive cell transfer therapy. *J Immunol* **191**, 2217-2225 (2013).

3. Joncker NT, Shifrin N, Delebecque F, Raulet DH. Mature natural killer cells reset their responsiveness when exposed to an altered MHC environment. *J Exp Med* **207**, 2065-2072 (2010).

4. Ardolino M, *et al.* Cytokine therapy reverses NK cell anergy in MHC-deficient tumors. *J Clin Invest* **124**, 4781-4794 (2014).

5. Schreiber RD, Old LJ, Smyth MJ. Cancer immunoediting: integrating immunity's roles in cancer suppression and promotion. *Science* **331**, 1565-1570 (2011).

6. Shifrin N, Raulet DH, Ardolino M. NK cell self tolerance, responsiveness and missing self recognition. *Sem Immunol* **26**, 138-144 (2014).

7. Fauci AS, Mavilio D, Kottilil S. NK cells in HIV infection: paradigm for protection or targets for ambush. *Nat Rev Immunol* **5**, 835-843 (2005).

8. Kumar V, McNerney ME. A new self: MHC-class-I-independent natural-killer-cell self-tolerance. *Nat Rev Immunol* **5**, 363-374 (2005).

9. Liao N-S, Bix M, Zijlstra M, Jaenisch R, Raulet D. MHC class I deficiency: susceptibility to natural killer (NK) cells and impaired NK activity. *Science* **253**, 199-202 (1991).

10. Pesce S, *et al.* Identification of a Subset of Human NK Cells Expressing High Levels of PD-1 Receptor: A Phenotypic and Functional Characterization. *J Allergy Clin Immunol*, (2016).

11. Zeestraten E, *et al.* Combined analysis of HLA class I, HLA-E and HLA-G predicts prognosis in colon cancer patients. *British journal of cancer* **110**, 459-468 (2014).

12. Sakuishi K, Apetoh L, Sullivan JM, Blazar BR, Kuchroo VK, Anderson AC. Targeting Tim-3 and PD-1 pathways to reverse T cell exhaustion and restore anti-tumor immunity. *J Exp Med* **207**, 2187-2194 (2010).

13. Fourcade J, *et al.* Upregulation of Tim-3 and PD-1 expression is associated with tumor antigen–specific CD8+ T cell dysfunction in melanoma patients. *J Exp Med* **207**, 2175-2186 (2010).

14. Jin H-T, *et al.* Cooperation of Tim-3 and PD-1 in CD8 T-cell exhaustion during chronic viral infection. *Proc Natl Acad Sci USA* **107**, 14733-14738 (2010).

15. Rizvi NA, *et al.* Activity and safety of nivolumab, an anti-PD-1 immune checkpoint inhibitor, for patients with advanced, refractory squamous non-small-cell lung cancer (CheckMate 063): a phase 2, single-arm trial. *The Lancet Oncology* **16**, 257-265 (2015).

16. Fourcade J, *et al.* PPD-1 and Tim-3 regulate the expansion of tumor antigen-specific CD8+ T cells induced by melanoma vaccines. *Cancer Res*, canres. 2908.2013 (2013).

17. Ott PA, Hodi FS, Robert C. CTLA-4 and PD-1/PD-L1 blockade: new immunotherapeutic modalities with durable clinical benefit in melanoma patients. (ed^(eds). AACR (2013).

18. Topalian SL, *et al.* Safety, activity, and immune correlates of anti–PD-1 antibody in cancer. *New England Journal of Medicine* **366**, 2443-2454 (2012).

19. Rizvi NA, *et al.* Mutational landscape determines sensitivity to PD-1 blockade in non–small cell lung cancer. *Science* **348**, 124-128 (2015).

20. Ahmadzadeh M, *et al.* Tumor antigen–specific CD8 T cells infiltrating the tumor express high levels of PD-1 and are functionally impaired. *Blood* **114**, 1537-1544 (2009).

21. Gordon SR, *et al.* PD-1 expression by tumour-associated macrophages inhibits phagocytosis and tumour immunity. *Nature* **545**, 495-499 (2017).

22. Benson DM, *et al.* The PD-1/PD-L1 axis modulates the natural killer cell versus multiple myeloma effect: a therapeutic target for CT-011, a novel monoclonal anti–PD-1 antibody. *Blood* **116**, 2286-2294 (2010).

23. Ndhlovu LC, *et al.* Tim-3 marks human natural killer cell maturation and suppresses cell-mediated cytotoxicity. *Blood* **119**, 3734-3743 (2012).

24. da Silva IP, *et al.* Reversal of NK-cell exhaustion in advanced melanoma by Tim-3 blockade. *Cancer Immunol Res* **2**, 410-422 (2014).

25. Pesce S, *et al.* Identification of a Subset of Human NK Cells Expressing High Levels of PD-1 Receptor: A Phenotypic and Functional Characterization. *J Allergy Clin Immunol* **139**, 335-346. e333 (2017).

26. Wherry EJ. T cell exhaustion. *Nat Immunol* **12**, 492-499 (2011).

27. Vivier E, Ugolini S, Blaise D, Chabannon C, Brossay L. Targeting natural killer cells and natural killer T cells in cancer. *Nat Rev Immunol* **12**, 239-252 (2012).

28. Smyth MJ, Hayakawa Y, Takeda K, Yagita H. New aspects of natural-killer-cell surveillance and therapy of cancer. *Nature Reviews Cancer* **2**, 850-861 (2002).

29. Atkins MB, Regan M, McDermott D. Update on the role of interleukin 2 and other cytokines in the treatment of patients with stage IV renal carcinoma. *Clin Cancer Res* **10**, 6342S-6346S (2004).

30. Spolski R, Leonard WJ. Interleukin-21: a double-edged sword with therapeutic potential. *Nature reviews Drug discovery* **13**, 379-395 (2014).

31. Leonard WJ, Wan C-K. IL-21 Signaling in Immunity. *F1000Research* **5**, (2016).

32. Elsaesser H, Sauer K, Brooks DG. IL-21 is required to control chronic viral infection. *Science* **324**, 1569-1572 (2009).

33. Fröhlich A, *et al.* IL-21R on T cells is critical for sustained functionality and control of chronic viral infection. *Science* **324**, 1576-1580 (2009).

34. John SY, Du M, Zajac AJ. A vital role for interleukin-21 in the control of a chronic viral infection. *Science* **324**, 1572-1576 (2009).

35. Takaki R, *et al.* IL-21 enhances tumor rejection through a NKG2D-dependent mechanism. *J Immunol* **175**, 2167-2173 (2005).

36. Brady J, Hayakawa Y, Smyth MJ, Nutt SL. IL-21 induces the functional maturation of murine NK cells. *J Immunol* **172**, 2048-2058 (2004).

37. Kasaian MT, *et al.* IL-21 limits NK cell responses and promotes antigen-specific T cell activation: a mediator of the transition from innate to adaptive immunity. *Immunity* **16**, 559-569 (2002).

38. Strengell M, *et al.* IL-21 in synergy with IL-15 or IL-18 enhances IFN-γ production in human NK and T cells. *J Immunol* **170**, 5464-5469 (2003).

39. Wan C-K, *et al.* Opposing roles of STAT1 and STAT3 in IL-21 function in CD4+ T cells. *Proc Natl Acad Sci USA* **112**, 9394-9399 (2015).

40. Sutherland AP, Joller N, Michaud M, Liu SM, Kuchroo VK, Grusby MJ. IL-21 promotes CD8+ CTL activity via the transcription factor T-bet. *J Immunol* **190**, 3977-3984 (2013).

41. Zeng R, Spolski R, Casas E, Zhu W, Levy DE, Leonard WJ. The molecular basis of IL-21–mediated proliferation. *Blood* **109**, 4135-4142 (2007).

42. Rao RR, Li Q, Bupp MRG, Shrikant PA. Transcription factor Foxo1 represses T-bet-mediated effector functions and promotes memory CD8+ T cell differentiation. *Immunity* **36**, 374-387 (2012).

43. Staron MM, *et al.* The transcription factor FoxO1 sustains expression of the inhibitory receptor PD-1 and survival of antiviral CD8+ T cells during chronic infection. *Immunity* **41**, 802-814 (2014).

44. Chung Y, *et al.* CD1d-restricted T cells license B cells to generate long-lasting cytotoxic antitumor immunity in vivo. *Cancer Res* **66**, 6843-6850 (2006).

45. Ko HJ, Lee JM, Kim YJ, Kim YS, Lee KA, Kang CY. Immunosuppressive myeloid-derived suppressor cells can be converted into immunogenic APCs with the help of activated NKT cells: an alternative cell-based antitumor vaccine. *J Immunol* **182**, 1818-1828 (2009).

46. Kim E-K, *et al.* Tumor-Derived Osteopontin Suppresses Antitumor Immunity by Promoting Extramedullary Myelopoiesis. *Cancer Res* **74**, 6705-6716 (2014).

47. Kim E-K, *et al.* Enhanced antitumor immunotherapeutic effect of B-cell-based vaccine transduced with modified adenoviral vector containing type 35 fiber structures. *Gene Ther* **21**, 106-114 (2014).

48. Richter J, *et al.* Clinical regressions and broad immune activation following combination therapy targeting human NKT cells in myeloma. *Blood* **121**, 423-430 (2013).

49. Pitt JM, *et al.* Dendritic cell-derived exosomes for cancer therapy. *J Clin Invest* **126**, 1224 (2016).

50. Jiang K, *et al.* Pivotal role of phosphoinositide-3 kinase in regulation of cytotoxicity in natural killer cells. *Nat Immunol* **1**, 419-425 (2000).

51. Coquet JM, *et al.* IL-21 is produced by NKT cells and modulates NKT cell activation and cytokine production. *J Immunol* **178**, 2827-2834 (2007).

52. Cui J, *et al.* Requirement for Vα14 NKT cells in IL-12-mediated rejection of tumors. *Science* **278**, 1623-1626 (1997).

53. Huang S, *et al.* Immune response in mice that lack the interferon-gamma receptor. *Science* **259**, 1742-1745 (1993).

54. Deng Y, *et al.* Transcription factor Foxo1 is a negative regulator of natural killer cell maturation and function. *Immunity* **42**, 457-470 (2015).

55. Beldi-Ferchiou A, *et al.* PD-1 mediates functional exhaustion of activated NK cells in patients with Kaposi sarcoma. *Oncotarget*, (2016).

56. Guillerey C, Huntington ND, Smyth MJ. Targeting natural killer cells in cancer immunotherapy. *Nat Immunol* **17**, 1025-1036 (2016).

57. Martinez GJ, *et al.* The transcription factor NFAT promotes exhaustion of activated CD8+ T cells. *Immunity* **42**, 265-278 (2015).

58. Roda JM, Parihar R, Lehman A, Mani A, Tridandapani S, Carson WE. Interleukin-21 enhances NK cell activation in response to antibody-coated targets. *J Immunol* **177**, 120-129 (2006).

59. Jeong WI, Park O, Radaeva S, Gao B. STAT1 inhibits liver fibrosis in mice by inhibiting stellate cell proliferation and stimulating NK cell cytotoxicity. *Hepatology* **44**, 1441-1451 (2006).

60. Gotthardt D, *et al.* Loss of STAT3 in murine NK cells enhances NK cell–dependent tumor surveillance. *Blood* **124**, 2370-2379 (2014).

61. Wei S, *et al.* Control of lytic function by mitogen-activated protein kinase/extracellular regulatory kinase 2 (ERK2) in a human natural killer cell line: identification of perforin and granzyme B mobilization by functional ERK2. *J Exp Med* **187**, 1753-1765 (1998).

62. Vivier E, Nunès JA, Vély F. Natural killer cell signaling pathways. *Science* **306**, 1517-1519 (2004).

63. Carreno BM, *et al.* A dendritic cell vaccine increases the breadth and diversity of melanoma neoantigen-specific T cells. *Science* **348**, 803-808 (2015).

64. Zhu EF, *et al.* Synergistic innate and adaptive immune response to combination immunotherapy with anti-tumor antigen antibodies and extended serum half-life IL-2. *Cancer cell* **27**, 489-501 (2015).

65. Kranz LM, *et al.* Systemic RNA delivery to dendritic cells exploits antiviral defence for cancer immunotherapy. *Nature*, (2016).

66. Moynihan KD, *et al.* Eradication of large established tumors in mice by combination immunotherapy that engages innate and adaptive immune responses. *Nat Med*, (2016).

국문 초록

암세포는 체내 면역 세포인 T 세포에 의해서 제거될 수 있지만, 암세포가 성장하고 전이됨에 따라 암세포 표면의 주 조직성 복합체 I (MHC class I) 이 감소 혹은 결핍되어 T 세포에 의해 제거되지 못한다는 것이 알려져 있다. 이러한 MHC class I 이 감소/결핍된 암세포는 체내의 자연 살해 세포 (NK cell)에 의해서 제거될 수 있다. 그러나 실제 암환자의 경우, NK cell 이 충분히 존재 함에도 불구하고, MHC class I 이 감소/결핍되어 있는 암세포가 제거되지 못하는 것이 보고 되고 있다. 본 연구는 이미 본 연구실에서 구축한 항암 면역치료백신인 BVAC 의 항암 면역효과를 분석하던 중, MHC class I 이 없는 암세포에의 효능 및 작용 기전을 밝히기 위해 진행되었다.

MHC class I 이 결핍된 암 세포주를 제작하여 BVAC 의 항암효과를 확인했을 때, NK cell 에 의해 효과적으로 MHC class I 이 결핍된 암의 성장을 억제하였다. 이에 본인은 BVAC 에 의해 MHC class I 결핍 암 환경에서의 NK cell 의 기능 저하가 회복될 수 있다는 가설을 세우고 실험을 진행하였다. 첫번째로, MHC class I 결핍 암 환경에서 NK cell 의 기능저하가 일어나는지 여부를 실험하던 중, MHC class I 결핍 암이 직접적으로 Programmed cell Death-1 (PD-1) 과 T cell immunoglobulin and mucin domain-3 (Tim-3) 분자를 NK cell 표면에 유도하는 것을 최초로 확인하였다.

두번째로, PD-1^+ Tim-3^+ NK cell 의 기능이 저하되어 있었고, 이런 기능저하는 BVAC 에 의해 자극되는 자연 살해 T 세포의 IL-21 분비에 의해 회복되는 것을 확인하였다. 뿐만 아니라 IL-21 의 직접적인 처리가 PD-1^+ Tim-3^+ NK cell 의 기능을 회복시키는 것을 여러 마우스 실험 모델을 통해 확인할 수 있었다. 세번째로, 기능 회복 기전은 STAT1 과 PI3K-AKT-FOXO1 신호체계를 통해 이루어지는 것을 밝혔다.

추가적으로 여러 종류의 암 환자의 암 조직을 얻어 암세포 표면의 MHC class I 이 정상세포에 비해 저하되어 있는 것과, 암세포에 침투된 NK cell 표면에 Tim-3 와 PD-1 분자를 발현하는 것을 확인하였다. 또한 이런 PD-1^+ Tim-3^+ NK cell 의 기능이 저하되어 있고, IL-21 에 의해서 기능이 회복된다는 것을 확인하였다. 따라서 본 연구를 통해 전이/말기 암에서 주로 발생하는 MHC class I 감소/결핍 암 세포는 IL-21 에 의한 기능 저하된 NK cell 의 기능 회복을 통해 제거 될 수 있다는 것을 밝힐 수 있었다.

주요어: 자연살해세포, IL-21, MHC class I, 면역 회피, 기능저하,
학번: 2012-24146